ULTRASOUND IMAGING TECHNOLOGIES FOR BREAST CANCER DETECTION AND MANAGEMENT – A REVIEW

Rongrong Guo, MD[1,2], **Guolan Lu, PhD**[3], and **Baowei Fei, PhD, EngD**[1,3,4,5,*]

[1]Department of Radiology and Imaging Sciences, Emory University School of Medicine, Atlanta, GA 30329

[2]Department of ultrasound, Shanxi Provincial Cancer Hospital, Taiyuan, Shanxi, China 030013

[3]The Wallace H. Coulter Department of Biomedical Engineering, Emory University and Georgia Institute of Technology, Atlanta, GA 30329

[4]Department of Mathematics and Computer Science, Emory College of Emory University, Atlanta, GA 30329

[5]Winship Cancer Institute of Emory University, Atlanta, GA 30329

Abstract

Ultrasound imaging is a commonly used modality for breast cancer detection and diagnosis. In this review we summarize ultrasound imaging technologies and their clinical applications for the management of breast cancer patients. The technologies include ultrasound elastography, contrast-enhanced ultrasound, three-dimensional ultrasound, automatic breast ultrasound, and computer-aided detection of breast ultrasound. We summarize the study results seen in the literature and discuss their future directions. We also provide a review of ultrasound-guided, breast biopsy and the fusion of ultrasound with other imaging modalities, especially magnetic resonance imaging (MRI). For comparison, we also discuss the diagnostic performance of mammography, MRI, PET, and CT for breast cancer diagnosis at the end of this review. New ultrasound imaging techniques, ultrasound–guided biopsy, and the fusion of ultrasound with other modalities provide important tools for the management of breast patients.

Keywords

Breast cancer; ultrasound imaging; ultrasound–guided biopsy; computer-aided detection

---

*Corresponding author: Baowei Fei, Ph.D., Eng.D., Department of Radiology and Imaging Sciences, Emory University School of Medicine, 1841 Clifton Road NE, Atlanta, GA 30329, bfei@emory.edu, Phone: 404-712-5649, https://fei-lab.org/baowei-fei/.

INTRODUCTION

Breast cancer is the most frequently diagnosed cancer and the leading cause of cancer death among females worldwide (Torre, et al. 2015). Among women in the United States, breast cancer has the highest incidence of all cancers and is the second most common cause of cancer death after lung cancer (Siegel, et al. 2015). It is estimated that there were 252,710 new cases (30% in all cancers) and 40,610 deaths (14% in all cancers) of breast cancer in females of the Unites States in the year 2017(Siegel, et al. 2017). A woman living in the United States has a 12.3% or a 1-in-8 lifetime risk of being diagnosed with breast cancer (DeSantis, et al. 2014). Early diagnosis is important for both treatment and the prognosis. Patients with smaller primary cancers at the time of their diagnosis had a significantly higher survival rate and a significantly reduced probability of dying from their cancer (Duncan and Kerr 1976). Early detection of breast cancer and accurate assessment of lesions are the goals of various image modalities. As a conventional, medical imaging modality, ultrasound (US) has had a very important role in breast cancer detection, image-guided biopsy, and lymph-node diagnosis for many years.

We conducted the literature search within the PubMed database using the keywords: "Breast" and "Ultrasound" in the title field plus "Cancer" and "Ultrasound" in the Abstract/ Title filed and with dates from 1996 to 2017. We also used the Google Scholar database for additional literature search. After reading the abstracts, we manually selected the relevant papers for this review. Each cited study had the IRB/ IACUC approval which was part of the search criteria. In this review, we begin with the explanation of various ultrasound techniques, including the ultrasound elastography technique, contrast–enhanced ultrasound, three-dimensional ultrasound, automatic breast-volume scanning, and computer-aided detection of breast cancer. We then provide an overview of ultrasound- guided breast biopsy and summarize ultrasound fusion with other imaging modalities navigation systems. We also review the performance of various imaging modalities for breast-lesion detection and lymph-node diagnosis. Finally, we conclude with discussions and future directions.

ULTRASOUND IMAGING TECHNIQUES FOR BREAST CANCER DETECTION

Breast ultrasound imaging in the clinic

Ultrasound can assess the morphology, orientation, internal structure, and margins of lesions from multiple planes with high resolution both in predominantly fatty breasts and dense, glandular structures. The general criteria for breast cancer detection with ultrasound are listed in Table 1. Among those characteristics, surrounding tissue, shape, margin contour, lesion boundary, and posterior acoustic features were significant factors to consider when classifying a lesion. Ultrasound has been used to classify benign, solid lesions with a negative predictive value of 99.5% (Stavros, et al. 1995). The measurement results of tumor, including the "halo", predicted tumor size for invasive lobular carcinoma, with a high diagnostic accuracy (Skaane and Skjorten 1999). The Breast Imaging Report and Data System (BI-RADS) of the American College of Radiology (ACR) (Radiology 2015) has been widely used in most of the countries where breast cancer screening is implemented. BI-RADS is designed to reduce variability between radiologists when creating reports for mammography, ultrasonography or MRI. The fourth version of the American Edition (2003)

is completed by ultrasonography and MRI lexicons. As an extensive update of the Fourth Edition, the BI-RADS Fifth Edition (2013) made some revisions based on accumulated clinical practice. Observer variability of BI-RADS for breast ultrasound (Lee, et al. 2008) showed that inter- and intra-observer agreement with the BI-RADS Lexicon for US is satisfactory. The use of the BI-RADS Lexicon can provide an accurate and consistent description and assessment of breast US. BI-RADS is integrated in the standard DICOM and is implemented directly on the digital mammography stations and in the computer-aided diagnosis (CAD) (Balleyguier, et al. 2007).

Ultrasound elastography

Elasticity is a property of a substance. Deformation occurs when the body is subjected to external forces and the original shape or size is restored upon removal of the external force. The slight deformation of tissue can be followed and marked by the speckle, ubiquitous, and low attenuation of ultrasound images. Echo data is acquired by the high speed of ultrasound to observe the tissue displacement (Bamber, et al. 2013). Elastosonography has become a routine tool in ultrasonic diagnosis which could measure the consistency or hardness of the tissues noninvasively in order to differentiate benign from malignant breast lesions.

Different categories for various elastographic techniques: Many different elastography techniques are available to measure and display elastography qualitatively or quantitatively using the displayed modus and different forces. Commonly used techniques are strain elastography (SE), acoustic radiation force impulse imaging (ARFI), transient elastography (TE), point shear-wave elastography (pSWE) and shear-wave elastography (SWE). According to the property displays there are three types, i.e. strain or strain rate, displacement, and shear wave speed. Strain elastography calculates and displays tissue strain; acoustic radiation force impulse imaging detects and displays tissue displacement; transient elastography and point shear-wave elastography records the shear-wave propagation speed (without making an image); and shear-wave elastography displays images of shear-wave speed (Bamber, et al. 2013). There are two types of applied forces in elastography, i.e. quasi-static, e.g. by probe palpation, and dynamic, e.g. by thumping, vibrating, acoustic radiation force. Quasi-static force is induced mechanically, while dynamic force could be induced by ultrasound. Shear-wave elastography is quantitative and its applied force is a dynamic force and needs to create shear. Other methods can use dynamic power, but can also use static or quasi-static force. Ultrasound-based elastography is created by a focused US impulse that transmits ultrasound pulses at a high speed from the same transducer and without compressing the skin. ARFI and SWE are both based on an acoustic force created by the focused US impulse.

Strain elastography: principle and applications: Strain elastography uses a hand-held probe with a slightly longitudinal pressing method or respiratory movement and obtains the hardness response information by estimating the deformation along the longitudinal axis and the strain distribution of the internal tissue. Strain elastography technology can be used to qualitatively and semi-quantitatively study the elastic strain rate ratio of a lesion with that of the surrounding normal tissue. Compression technology is easy to implement, although it suffers from a higher operator dependence and poor reproducibility. Real-time elastography

(RTE), which generates "strain imaging" by compression, assesses the relative elasticity of the tissue in a specific area of interest creating an elastogram, i.e. a color-coded map, that is superimposed on the US image. The relative elasticity may vary according to the studied tissues, the size of the RTE-box and the exerted pressure. As tissue is mechanically nonlinear, the strain from a given force decreases with increasing force and the tissue becomes harder as more force is applied. The resolution of strain image changes with different contrast discrimination of the strain and also changes with the window sizes or displacement, strain estimators and the smoothing window, palpation speed and amplitude, persistence, etc. There are some artifacts that may influence the strain images, such as friction between the transducer and skin which could decrease the strain of surface tissue; a narrow compressor which generates limited strain with poor homogeneity and decays rapidly with depth; the artifact of strains concentration which might be seen when there is a hard inclusion in a soft background and which can explain the high strain at slip boundaries and edge enhancement; and the "egg shell" which might occur when soft regions are buried in a stiff background as stiff tissue prevents the generation of strain inside the egg. The procedures which help generate good strain images include: close to the target; and some distance to tissue boundaries, anatomical plane and other structures.

The investigation of 169 *ex vivo* breast tissue samples (Samani, et al. 2007) showed that the elastic modulus of normal breast fat and fibroglandular tissue are similar while fibroadenomas were approximately twice as stiff. Fibrocystic disease and malignant tumors exhibited a 3–6-fold increased stiffness while high-grade, invasive ductal carcinoma exhibited up to a 13-fold increase in stiffness compared to fibroglandular tissue (Samani, et al. 2007). A five-point scale was adopted according to the hardness of nodules in strain elastography (Itoh, et al. 2006). Score 1 indicates deformability of the entire lesion; score 2 indicates deformability of most of the lesion with some small, stiff areas; score 3 indicates deformability of the peripheral portion of a lesion with stiff tissue in the center; score 4 indicates that the entire lesion is stiff; and score 5 indicates that the entire lesion and surrounding tissue are stiff. A lesion scoring from 1 to 3 points was considered benign (Figure 1), while that scoring at 4 or 5 points was malignant. According to the 10 largest published studies with the five-point scale and a cut-off value between 3 and 4 for assessing malignancy, Carlsen (Carlsen, et al. 2013) presented the comparison of the diagnostic performance between the SE and B-mode. All of eight studies showed a better sensitivity for B-mode than for SE, while seven of these studies showed better specificity and higher accuracy for SE than for B-mode imaging; combined B-mode and SE sensitivity decreased in three of five studies, while specificity and accuracy increased in four of five studies.

Acoustic radiation force impulse Imaging (ARFI): ARFI employs a short acoustic impulse of high intensity to display displacement of tissue elements in a longitudinal direction and qualitatively creates a static map of the relative stiffness of the tissues within a small box. The tissue displacement can be accessed according to the area ratio (Li, et al. 2015). Compared to strain elastography, ARFI imaging has better resolution, less inter-observer variability, and less influence by the stress concentration and by slip movement anterior to the imaged region, and exhibits a better image in deep tissue. However, the ARFI method can only create static images and not dynamic sequences, such as strain images, and

it also depends on absorption and reflection of the pushing beam and delay between the push and the displacement measurement. ARFI mentioned above refers to the acoustic radiation force impulse imaging (virtual tissue imaging, VTI). In some literature studies the point shear-wave elastography (pSWE) is referred to as ARFI quantification, i.e. virtual touch tissue quantification, VTQ, and which has been used for the method where a regional average of only shear-wave speed is measured using radiation force excitation (Bamber, et al. 2013). The quantitative method employs a primary acoustic impulse focused on a region of interest where it generates pressure waves in transverse propagation in order to deform the tissues. The primary impulse is followed by a few, interrogating impulses distributed in the surrounding tissues and designed to calculate the propagation velocity of pressure waves. The propagation velocity and attenuation of the waves are related to the stiffness and visco-elasticity of the tissue. The waves travel faster in stiff tissues than in non-stiff tissues. This quantitative method provides pressure-wave velocity but no spatial distribution.

According to a meta-analysis (Li, et al. 2015) ARFI elastography seems to be a good method for differentiating between benign and malignant breast lesions. The cut-off values for the shear-wave velocity of VTQ ranged widely from 2.89 to 6.71 m/s, while the VTI area ratio only ranged from 1.37 to 1.66. The values of the total sensitivity and specificity were 0.843 and 0.932 for the VTQ of ARFI and 0.864 and 0.882 for the VTI of ARFI, respectively (Li, et al. 2015). According to other published studies, the mean VTI area ratio of the benign lesions of 1.08 ± 0.21 differed from that of the malignant lesions of 1.99 ± 0.63(Meng, et al. 2011), while the mean shear-wave velocity differed from 4.49 to 8.22 ± 1.27 m/s in malignant lesions and from 2.25 ± 0.59 m/s to 3.25 ± 2.03 m/s in benign lesions (Bai, et al. 2012, Meng, et al. 2011, Tozaki, et al. 2011).

Shear-wave elastography: A varying pressure applied to tissue surface generates shear deformation as well as longitudinal propagation. The propagate wave of shear deformation is utilized in sonography to obtain elastic information regarding tissue. Shear-wave elastography (SWE) uses acoustic radiation force to obtain real-time 2D or 3D quantitative shear-wave speed images. The speed of shear-wave propagation is proportional to the Young modulus (kilopascals, kPa), a measure of the resistance of tissue to shearing, and which is currently used to quantitatively measure lesion elasticity (Athanasiou, et al. 2010, Evans, et al. 2010). The image is a semitransparent, color overlap on a B-mode image in a region of interest, and which represents the distribution according to the local propagation velocity of the pressure waves. Values of the maximum and average stiffness and the standard deviation can also be measured. SWE is quantitative and displays no stress concentration with less operator dependence. High pre-stress will cause a high SWE artifact in superficial tissue. The shear-wave propagation near a boundary and thin layer might be invalid in order to assume the relationship between their speed and elastic modulus. As shear waves cannot propagate through pure fluid, SWE is sensitive to the average fluid content in tissue.

High mean stiffness values in shear-wave elastography have been shown to have a statistically significant positive association with the invasive size, high histologic grade, lymph-node involvement, tumor type, and vascular invasion for invasive breast cancer, and which suggests that higher mean stiffness values have poorer prognostic features (Evans, et al. 2012). The stiffness of malignant breast lesions may be influenced by the desmoplastic

reaction of intra- and extranodular infiltration of interstitial tissue or infiltration of the intraductal component, except in medullary and mucinous carcinomas (Goddi, et al. 2012). Wendie (Berg, et al. 2015) showed the median maximum stiffness (termed "Emax") on shear-wave elastography of breast disease of various histopathologic grades (Figure 2). SWE provides more information regarding unidentifiable breast lesions (Figure 3).On shear-wave elastography, Evans (Evans, et al. 2012) reported that invasive tumors smaller than 10 mm had a mean stiffness of 64 ± 23 (SD) kPa, that tumors between 10–20 mm had a stiffness of 129 ± 66 kPa, and that tumors larger than 20 mm had a stiffness of 156 ± 45 kPa.

Clinical applications of ultrasound elastography: Some clinical questions are worth noting: 1) Precompression is the amount of pressure applied during scanning. The precompression can change the tissue's elastic properties in shear-wave elastography. If enough precompression is applied, the elastographic properties of all tissues are similar (Barr 2012). With minimal precompression, the differences of shear-wave speed for different tissues are maximized. Only a minimal amount of precompression is required in order to obtain better quality elastogram, while a mild amount of precompression is needed to obtain better quality B-mode images. 2) Under some biological conditions shear waves cannot form an image, for example, if the shear-wave velocity is too high it cannot be caught in extremely stiff cancer. When the elasticity cannot be evaluated, the color display will turn off This display should differ from a low shear-wave elasticity of soft-tissue areas. As a cyst which is non-viscous liquid does not support shear waves, they appear as black color. 3) The direction of a probe may affect shear-wave velocity, and which should be considered in clinical application. 4) Shear-wave propagation is depth limited. If a lesion is deeper than 4 cm, it may not be possible to obtain a result. Repositioning the patient to make the lesion closer to the skin surface can help in these cases (Barr 2012). 5) The size of a mass influences the SWF result and it has been shown that smaller lesions have better sensitivity and specificity (Feng, et al. 2010, Giuseppetti, et al. 2005).

There has been controversy regarding the accuracy of breast ultrasound elastography compared to conventional B-mode Ultrasound, and SWE was not significantly more sensitive than grayscale ultrasound for the detection of either invasive ductal carcinoma or invasive lobular carcinoma (Sim, et al. 2015). However, elastography can lead to a re-evaluation of the lesion (Figure 4), and the lesions that appear even echoic on B-mode imaging may have different strain properties. Four of 52 cases of lobular cancers were benign on both mammography and grayscale ultrasound, but were suspicious on SWE (Sim, et al. 2015). The diagnostic accuracy of shear-wave elastography for solid breast lesions is at least as good as grayscale ultrasound with BI-RADS classification (Evans, et al. 2010). Elastosonography is a simple, fast, and non-invasive diagnostic method that may improve the SP of diagnostic breast cancer, especially for BI-RADS 3 (Scaperrotta, et al. 2008). A prospective study in 939 patients proved that adding quantitative SWE features to the BI-RADS feature in adjustment 3 and 4a class breast masses could improve the specificity of breast US mass assessment without loss of sensitivity (Berg, et al. 2012). Fausto used the strain ratio, the ratio of the glandular tissue and fat, and the ratio of the lesion and fat ratio to improve the diagnostic accuracy in BI-RADS 3 and 4 lesions (Fausto, et al. 2015).

Elastography has been found to reduce the need for benign biopsies when they are used as a complementary tool to conventional ultrasound (Lee, et al. 2013). Elastography could then help to define the location of a biopsy and characterize a complex lesion (Figure 4). A recent study showed that anisotropy in 2D shear-wave elastography is an indicator of breast cancer (Skerl, et al. 2016). A meta-analytic (Sadigh, et al. 2012) comparison of the elasticity and B-mode showed that the application of elastography as a single test is not superior to the B-mode alone, but that in low-risk patients it is recommended to perform an elastography following a positive B-mode result in order to decrease the rate of unnecessary biopsies.

Contrast-enhanced ultrasound

The tumor's vessel density is proportional to the tumor size and the pathological severity (del Cura, et al. 2005). The high density of blood vessels and vascular distribution disorders are present in breast malignant lesions. In order to visualize vascular structures and tissue with different vascularity, contrast-enhanced ultrasonography (CEUS) is used in clinical research (Kim, et al. 2003). CEUS utilizes intravenously injected gas microbubbles in order to improve backscattering from the vasculature (Calliada, et al. 1998). Microbubbles are specific gas encapsulated in various types of shells, with diameter sizes between 1 and 7 μm and more echogenic than red blood cells, and they are confined to intravascular spaces and do not leak through the vessel wall. SonoVue (Bracco Spa, Milan, Italy) ®, the commonly used contrast agent, is a blood–pool perfluora gas agent that consists of microbubbles of sulfur hexafluoride (SF_6) stabilized by a phospholipid shell. Due to differences in the acoustic impedance and compressibility between the microbubbles and surrounding media, ultrasound contrast agents mainly act as nonlinear scatters. Nonlinear imaging techniques, including pulse inversion harmonic imaging, intermittent power Doppler, and subharmonic imaging, are used to reduce bubble destruction and provide improved depiction of microvascularity. Microbubble contrast agents, combined with nonlinear imaging techniques, could demonstrate the vascular morphology.

CEUS offers qualitative and quantitative analysis for characterizing breast lesions. Following SonoVue ® administration, different perfusion phases could be identified, i.e. early (0–1 min), mid (1–4 min), and late (4–6 min) phases (Zhao, et al. 2010). CEUS dedicated software produced the following parameters on time/intensity (T/I) curves (Figures 5, 6): peak %; time to peak (TTP); mean transit time (MTT); regional blood volume (RBV); and regional blood flow (RBF). Enhancement patterns in the early phase and contrast medium persistence in the late phase differ in benign and malignant breast lesions. The features of malignancy include early and fast enhancement in the early phase, centripetal filling, claw-shaped enhancement, higher maximum intensity, and contrast medium accumulation in the late phase (see Figure 5), while the features of benign tissue include delayed, centrifugal filling, homogeneous enhancement, and seldom contrast medium present in the late phase (see Figure 6) (del Cura, et al. 2005) (Zhao, et al. 2010) (Balleyguier, et al. 2009) (Jung, et al. 2005).

Since 2011, the EFSUMB Guidelines of CEUS for the breast remains an important topic for research, but has not been recommended for routine clinical use (Piscaglia, et al. 2012). The research of Ricci et al. showed that the sensitivity and specificity of CEUS for differentiating

malignant from benign breast lesions are 100% and 87.5%, respectively, and contrast-enhanced sonographic patterns correlated well with those provided by MRI (Ricci, et al. 2007). The positive predictive value (PPV) of CEUS evaluation was 91%, and the negative predictive value (NPV) was 73% (Caproni, et al. 2010). The size of a breast lesion measured with CEUS is larger than that measured with conventional ultrasound. Pathologic examination of a mass with measurement discrepancy revealed primarily ductal carcinomas in situ (DCIS) (Figure 7), invasive carcinoma with a DCIS component, adenosis with lobular hyperplasia in breast cancers, and inflammatory cell infiltration in one granulomatous mastitis (Jiang, et al. 2007). A mass with a well-defined margin has only a small possibility to get larger measurements on CEUS. Doppler ultrasonography with contrast-agent injection is highly efficient and better for evaluating the response of neoadjuvant treatment and confirmation of tumor hypervascularised destruction before radiofrequency (RF) in local, recurrent breast cancer (Vallone, et al. 2005) (Lamuraglia, et al. 2005). Enhancement patterns and parameters of contrast-enhanced US may be useful in the noninvasive prediction of the prognostic factors of breast cancer (Wan, et al. 2012).

Three-dimensional ultrasound

Three-dimensional (3D) ultrasound may offer new perspectives in the field of breast ultrasound. There are two, main types of 3-D ultrasound. One is the use of 2-D imaging equipment with a certain mechanical movement to reconstruct the 3-D ultrasound volume. The other one is real-time volumetric echo which uses a matrix array transducer that electronically scans a 3-D volume. Replacing a single row of elements in conventional linear transducers, the elements in a matrix array transducer are arranged in a two-dimensional (2-D) grid. Matrix array generates a beam in both positions, and thus forming an entire, pyramid-shaped volume (Kisslo, et al. 2000). The probe was held still and patients were asked to stop breathing during the 1–3 s that the ultrasound unit required to generate the 3D volume. Then three perpendicular reconstructed planar sections, i.e. sagittal, transverse, and coronal planes, were displayed simultaneously on the ultrasound screen. The coronal reconstruction images can show the details of anatomy and spatial locations of a lesion and gland and thus potentially improve the characterization of breast lesions. A retraction phenomenon in the coronal plane of the 3D volume is the special characteristic of breast cancer (Figure 8). 3D ultrasound allows the calculation of the corresponding volume. At the same time, in 3D ultrasound the characteristics of the orientation, margin, margin contour, and surrounding tissue in the conventional planes are still significant and independent parameters (Watermann, et al. 2005).

A few preliminary studies have explored the use and advantages of contrast-enhanced 3-D US (3-D CEUS) in evaluating breast tumors (Forsberg, et al. 2004, Jia, et al. 2014, Sridharan, et al. 2015). Forsberg compared the diagnostic ability for breast cancer evaluation of 3-D US with 2-D US and 3-D power Doppler imaging, and showed that the areas under the receiver operating characteristic curve of 2-D CEUS imaging are 0.51 and 0.76 for 3-D CEUS, and when 3-D CEUS is combined with mammography it is 0.90 (Forsberg, et al. 2004); The 3-D CEUS score for tumor angiogenesis agreed with that of contrast-enhanced, magnetic resonance imaging (DCE-MRI) and correlated well with the biological factors, i.e. microvessel density (MVD), the vascular endothelial growth factor (VEGF), and matrix

metalloproteinases (MMP-2, MMP-9) expression (Jia, et al. 2014). Sridharan showed that contrast-enhanced, 3-D subharmonic US could quantitatively evaluate the variations of vascular heterogeneity for benign and malignant breast lesions, i.e. a benign lesion showed a significant difference in vascularity between the central and peripheral, while a malignant lesion had no difference (Sridharan, et al. 2015).

Automated breast sonography

Handheld US is limited by operator dependence, non-reproducibility, and its inability to image and store three-dimensional (3-D) volumes of the breast. To overcome these limitations, an automated breast ultrasound system (ABUS) has been developed. This modality makes it possible to simultaneously visualize large sections of the breast from the skin surface to the chest wall and to store entire breast volumes on a picture archiving and communication system, and thus enabling temporal comparison of current studies with relevant prior studies. In 2008, the SonoCine system received U.S. Food and Drug Administration (US FDA) approval (Shin, et al. 2015). US standard sensor mounts on an articulated arm and scans the entire breast while the operator can adjust the angle and pressure of the transducer. The imaging produces the same image as 2D hand scanning. This technique does not allow three-dimensional (3D) manipulation or reconstruction of the raw data. The imaging is reviewed in real time, as any standard US examination, either at the time of the examination or later if the examination was recorded and stored. In September 2012, Somo-v ABUS systems were approved by the US FDA to be used in women with dense breasts who have negative X-ray mammography results and have not undergone previous, invasive procedures. With this system, a larger transducer paddle (Figure 9) is placed over the breast with a small amount of compression applied in order to stabilize the breast, scan, and acquire the data (Shin, et al. 2015). The US transducer might have to be repositioned so as to cover the entire breast. 3D data reconstruction is made by computer algorithms. As the process of ABUS is without change and is automatic, it does not require highly trained specialists and can eliminate the fatigue of the technician. The acquisition time of ABUS is an average of 15 minutes for a patient with average- sized breasts (Shin, et al. 2015). It takes a proficient radiologist 3–10 minutes to interpret a case of ABUS results, depending on the complexity (Kaplan 2014). According to the ACRIN 6666 (American College of Radiology Imaging Network 6666) study, it takes a physician approximately 20 minutes to scan a full bilateral examination (O'Connell, et al. 2013). Gel pad application for automated breast sonography is easy and provides significant pain relief, with the scan coverage expanded, and the image quality maintained (Kim, et al. 2015). Due to its digital capability, each sectional plane of the saved volume can be visualized (Figure 10), thereby avoiding the investigator- dependent and non-standardized documentation.

Wenkel reported that HHUS and ABUS had good agreement (Kappa 0.83 –0.87) regarding the BI-RADS classification (Wenkel, et al. 2008). In screening, the diagnostic quality of ABUS is similar to that of hand-held ultrasonography (HHUS) (Stoblen, et al. 2011). The ABVS can provide more accurate information for assessing the extent and location of lesions than handheld US (Li, et al. 2013, Shin, et al. 2011). It could, therefore, improve the detection accuracy of invasive cancers less than or equal to 1 cm (Kelly and Richwald 2011). Adding ABUS to mammography has improved the callback rates, accuracy of breast cancer

detection, and confidence in callbacks for dense-breasted women (Kelly, et al. 2010). The accuracy, SE, and SP of ABUS for breast cancer diagnosis were 79.0%, 83.3%, and 78.1%, respectively (Wojcinski, et al. 2013). ABUS appears accurate in assessing the preoperative extent of pure ductal carcinoma in situ (DCIS) (Li, et al. 2013). ABUS can reliably detect additional, suspicious lesions identified on breast MRI and may help with the decision regarding the biopsy guidance method, i.e. US vs. MRI, as a replacement tool for hand-held, second-look ultrasound (Chae, et al. 2013). The large probe of ABUS provides the whole coverage and characterization of a large mass (Figure 11) and it might provide an accurate measurement of a cancerous tumor larger than 5 cm (Shin, et al. 2015). ABUS can help to demonstrate intraductal abnormalities and the extent of these abnormalities in the ductal system (Figure 12). Categorization of ultrasonographic findings using automated breast US are useful for predicting the likelihood of malignancy (Tozaki and Fukuma 2012). ABUS may have a role as a replacement tool for hand-held, second-look US (Chae, et al. 2013).

Computer-aided detection for breast ultrasound

Breast ultrasound imaging and diagnosis is highly operator-dependent and may have a high inter-observer variation rate. Moreover, with the large amount of data that needs to be analyzed when using automated 3D breast ultrasound, the risk of oversight errors is substantial. Therefore, computer-aided diagnosis (CAD) is desirable in order to help radiologists in breast cancer detection and classification. Computer-aided detection (CAD) may be used as a second reader to improve the radiologists' accuracy in distinguishing malignant from benign lesions on 2D and 3-D US volumetric images.

A CAD system generally consists of four stages, i.e. preprocessing, segmentation, feature extraction and selection, and classification. Interested readers are referred to a more detailed review in (Cheng, et al. 2010).

1)   Preprocessing: The main purpose of image preprocessing is to enhance the image and suppress specklewhile preserving important diagnostic features. Speckle noise reduction techniques generally involve filtering methods, wavelet domain methods, and compound approaches (Cheng, et al. 2010).

2)   Segmentation: Image segmentation separates objects from the background and allocates regions ofinterest for feature extraction. The techniques include histogram thresholding, the active contour model, Markov random field, and neural network. The active contour model combines prior knowledge regarding the relative smoothness of the 3D mass shape, as seen on the US volumetric image, with information in the image data in order to decrease the interference of image speckles, posterior shadowing, and variations of the gray level both within the mass and within the normal breast tissue. Sahiner (Sahiner, et al. 2007) designed a computer algorithm to automatically delineate mass boundaries and extract features on the basis of segmented mass shapes and margins of 3D US volumetric images.

3)   Feature extraction and selection: After mass segmentation, the features are extracted from a breastmalignant lesion and its margins for classification, including variance of intensities, entropy, average intensity, margin contrast,

volumetric height-to-width ratio, sphericity, compactness, posterior acoustic behavior, and speculation. These features can be divided into four categories, i.e. texture, morphological, model-based, and descriptor features. Most of these features are listed in the breast imaging report and data system. These features are also important for the design of CAD systems (Moon, et al. 2012). Features extracted from each different section were combined to define case-based features for a given mass. The case-based feature vectors were fed into classifiers, such as linear discriminant analysis, with stepwise feature selection in order to obtain computerestimated malignancy scores. It has been shown that texture features can distinguish malignant from benign lesions on 2-D US (Gomez, et al. 2012). Another study (Liu, et al. 2014) incorporated three, important types of texture features, including local binary patterns (LBPs), gray–level, co-occurrence matrix (GLCM)-based features, and the Gabor filters, in order to classify benign and malignant lesions in automated three-dimensional breast ultrasound images. LBP features from the area surrounding the segmented lesion, texture features of squares and autocorrelation, and texture features based on 3-D GLCM could be used to classify the ABUS volumes of a breast lesion (Liu, et al. 2014). The ranklet transform after texture features extracted may be useful for improving the ability to discriminate between triple-negative breast cancer and benign fibroadenomas (Hipwell, et al. 2016). The phased, congruency-based binary pattern (PCBP) is an oriented local texture descriptor that combines the phase congruency (PC) approach with the local binary pattern (LBP). Tao Tan (Tan, et al. 2015) used a large number of 2D, Haar-like features to differentiate lesion structures from false positives. Chang used neutrosophic image transformation and fuzzy c-mean clusterings to define the lower and upper boundaries of the fibroglandular tissue in US images and then extracted the number of hypoechoic regions and histogram features. The detection result of the proposed system showed high agreement with that of the radiologists (Chang, et al. 2015).

4)   Classification: The selected features were fed into a classifier in order to categorize the images intolesion/no-lesion or benign/malignant classes (Cheng, et al. 2010).The commonly used classifiers include linear classifiers, artificial neural networks, Bayesian neural networks, decision tree, support vector machine, and template matching. Hussain (Nagarajan, et al. 2013) proposed a method to classify mass regions by building an ensemble classifier that employs Gabor features and achieved the best result. Support vector machine (SVM) which utilizes a structure risk minimization to diminish the error of the learning machine and has been widely used for tumor classification (Cai, et al. 2015). Using a cascade of Gentle Boost classifier that combines these features can improve their previously developed CAD system in the initial candidate detection stage. A machine learning methodology involving pairing adaptive boosting with selective pruning achieved high diagnostic performance without the added cost of an additional reader for differentiating solid breast masses by ultrasound (Venkatesh, et al. 2015). A leave- one-case-out resampling method was used to train the classification system and to obtain the malignancy scores

(Sahiner, et al. 2007), and this method improved the radiologists' accuracy in distinguishing malignant from benign breast masses on 3D US volumetric images. Bhatti PT (Bhatti, et al. 2001) used speed-weighted pixel density to quantify vascularity in and around each mass and made the conclusion that combining the vascularity measure with age can improve the discrimination of sonographically detected breast masses.

A computer-aided diagnosis (CAD) system can help readers to assess the probability that a particular lesion is malignant. The average area under the ROC curve for radiologists using CAD for discriminating malignant masses from benign masses on 3D volumetric US images, was increased from 0.83 (range, 0.81–0.87) to 0.90 (range, 0.86–0.93) (Sahiner, et al. 2007). The CAD system improves the performance of less experienced readers for distinguishing malignant from benign lesions in ABUS (Tan, et al. 2013).

Summary and Future Directions

Breast cancer detection is a widely used application of ultrasound imaging in the clinic. Ultrasound elastography and contrast enhanced ultrasound provide additional information for breast lesion based on duplex sonography. Elastography imaging is a qualitative and quantitative technique regarding tissue stiffness or hardness rather than anatomy. However, elastography images cannot distinguish between lesions and surrounding tissue when their elasticity properties are the same. The quality of the elastography image is limited by the depth of a lesion. Combination of B-mode and elastography could overcome these problems. Uniform standards for elastography commercial systems and uniform clear classification for elastography commercial modes are needed. A convenient system for elastography information could make elastography more widely used in clinical practice regarding breast disease. Contrast-enhanced ultrasound displays the vascular structure and perfusion of breast tumors and provides quantitative parameters on the time/intensity curve, which are useful for discriminating between benign and malignant lesions and follow-up after local treatment. Automated breast US presents useful information regarding breast lesions, from their coronal reconstruction plane and the extensive field of transverse and sagittal planes, with the advantage of consistent acquisition images, being less time-consuming, and causing less fatigue to the operator. In the next section, we will continue to discuss about the use of ultrasound for image-guided biopsy of breast cancer.

ULTRASOUND IMAGE–GUIDED BIOPSY OF BREAST CANCER

Various biopsy methods for the breast

Image-guided breast biopsy is currently the gold standard for the pathologic evaluation of breast cancer. It can be performed safely and reliably with minimal invasiveness in clinical practice and with increased patient convenience and decreased cost (Roe, et al. 1997). Ultrasound, stereotactic mammography, magnetic resonance imaging (MRI), and positron emission mammography (PEM) are now successfully used for the guidance of the biopsy needle in order to obtain a proper tissue sample that can be histologically assessed. The choice of image guidance for biopsy is based on a variety of factors, including which modality best visualizes the lesion, the physician's clinical experience, patient comfort, cost,

ease of access, and equipment availability. The common methods of biopsy include fine-needle aspirate biopsy, vacuum-assisted biopsy, and core-needle biopsy. Meta-analysis for various diagnostic biopsy methods for women at average risk of cancer showed that SE estimates were higher than 0.90 and SP estimates were higher than 0.91 for all methods (Dahabreh, et al. 2014).

Fine–needle aspiration biopsy (FNAB) of the breast has been considered a reliable sampling and less invasive morphological diagnostic method. This method reduces health care costs and the psychological pressure for the patients. FNAB can be performed with freehand for breast lesions that are palpable and for non-palpable breast lesions it could be guided by ultrasound or mammography. Cytopathology for the small-sized samples obtained by fine-needle aspiration provide the necessary information, although it does not assess the tissue architecture. A prospective study involving palpable nodules with a diameter of more than 2 cm showed fine-needle aspiration cytology with an SE of 90.4% and core biopsy with an SE of 95.2% (Dennison, et al. 2003). In a blinded analysis, the SE of FNAB cytology was 92% and the SP was 83% (Reinikainen, et al. 1999). However, FNAB has the drawback of inadequate or non-diagnostic cytological samples and a high false–negative rate (Delle Chiaie and Terinde 2004).

Core-needle biopsy can be performed with an automated core-biopsy gun or a hand-held biopsy needle. Automated core needles have different sizes, i.e. 14-, 16-, and 18-gauge. The quantity and quality of breast biopsy specimens depend on the needle size. Among the three needle sizes, 14-gauge, long-throw biopsy needles may provide the highest quality core samples for breast biopsy (Helbich, et al. 1998). The samples are sent for histological examination which is considered to be more reliable than fine-needle aspiration. Because core-needle biopsy samples only part of the breast abnormality, it seems to have a lower risk of complications than open surgical biopsy. The incidence of severe complications with core needle biopsy was less than 1 percent. The adverse events include hematomas, bleeding, vasovagal reactions, and infections. The percentage of patients experiencing any of these adverse events was less than 1.5 percent (Dahabreh, et al. 2014). There are potential risks of displacement of cancerous cells during biopsy, however, the clinical significance of these findings is unclear and tumor development on the biopsy-needle track is extremely rare.

Vacuum-assisted biopsy (VAB) was performed with an 11-G needle or a 10-G needle (Mammotome or EnCore or other Breast Biopsy System). In the review of the Brown Evidence-based Practice Center, vacuumassisted biopsy is also included to core-needle biopsy(Dahabreh, et al. 2014). Once it is inserted and rotated in the sampling chamber, tissue samples are captured from different areas of the lesion that is double the size of those obtained by conventional core needle biopsy. It can be used to remove a small, benign lesion and decrease the underestimation of atypical ductal hyperplasia (ADH) and ductal carcinoma in situ (DCIS) (Burbank 1997). The core biopsy and VAB system are usually guided by stereotactic mammography or ultrasound. The differences in SE and SP between US-guided automated and vacuum-assisted are 0.01 and -0.01(Dahabreh, et al. 2014).

Ultrasound and stereotactic mammographic-guided biopsy

Ultrasound-guided biopsy is easy to perform and radiation-free. Operators can observe the plane and the angle between the lesion and the needle in real-time and verify and flexibly adjust the direction of the needle position (Liberman, et al. 1998, Parker, et al. 1993). A new needle guidance system was developed that coupled the transducer with three, rotational joints in order to eliminate the need to align the ultrasound scanning plane with the needle and displayed the needle trajectory before the insertion so that the participant could focus solely on the guidance of the needle toward the intended target lesion (Bluvol, et al. 2009). Sometimes 2D ultrasound is misleading with the artefactual appearance of the correct needle placement when it is positioned at the edge of a lesion. This inaccurate information can be compensated for with 3D ultrasound. The advantages of 3D ultrasound validation include a reduction in the number of core samples required in order to achieve a reliable histological diagnosis and a possible reduction in the risk of tumor cell displacement (Delle Chiaie and Terinde 2004, Smith, et al. 2001). A retrospective study showed the false-negative of US-guided 14-gauge CNBs for breast lesions rate was 2.0% with a sensitivity of 95.4%(Jung, et al. 2017).

Stereotactic mammographic biopsy accounts for nearly half of all image-guided biopsies. Stereotactic mammographic biopsy is suitable for micro-calcifications, distortions, and focal densities, but it is limited by weight and breast thickness restrictions. Keranen demonstrated that the accuracy and clinical usefulness of vacuum-assisted biopsy using US guidance for breast micro-calcifications was comparable to stereotactic guidance (Keranen, et al. 2015). Radiological stereotactic and sonograms can also be used for preoperative localization by wire. Percutaneous biopsy of a non-palpable breast mass using either US or stereotactic guidance is less expensive than surgery and the cost savings are greater than with US-guided biopsy (Liberman, et al. 1998).

Summary and Future Directions

Image-guided biopsy is another important application of ultrasound techniques in addition to detection of breast cancers. Ultrasound-guided biopsy provides gold standard for pathological diagnosis and treatment selection. Since different imaging techniques may have complementary roles, combination of ultrasound with different imaging modalities could further improve biopsy accuracy in the future. In the following section, we will discuss about the combination of ultrasound with MRI, PET, CT, and Mammography for breast cancer diagnosis and biopsy.

COMBINATION OF ULTRASOUND WITH MRI, PET, CT OR MAMMOGRAPHY

Ultrasound–MRI fusion-guided diagnosis

Due to the high SE (Harms, et al. 1993) of breast MRI and the flexibility of US, research regarding the integration of sensitive MRI and real-time ultrasound has been conducted for many years (Curiel, et al. 2007). In 2000, it was reported (Obdeijn, et al. 2000) that the combined approach of MR imaging, sonography, and aspiration fine-needle cytology is a good alternative to the MR imaging–guided biopsy for revealing unknown primary sites in women with axillary lymph-node metastases from adenocarcinoma. In this section we will

discuss ultrasound fusion with MRI diagnosis for breast cancer, including second-look ultrasound and the ultrasound combined with supine–MRI fusing volume navigation technique.

Second- look ultrasound: Second-look US (SLUS) is an additional, targeted breast imaging examination in which the lesions found on MR images can be located by SLUS and can be histologically clarified by US-guided biopsy. The term, second-look, is used even when there is no initial US examination. Regardless of whether antecedent, bilateral, whole-breast US is performed, SLUS is usually recommended before MR imaging–guided biopsy. Spick's study demonstrated the variable utility of SLUS in MR imaging–detected lesions and showed that 57% (22.6%- 82.1%) of MRI lesions can be located by SLUS and can be histologically clarified by US-guided biopsy (Spick and Baltzer 2014). SLUS more frequently detected foci (67%) and masses (73%) than it did non-mass-like lesions (54%). Rim enhancement in masses and clumped enhancement in non-mass lesions were also significantly more likely to have an ultrasound correlate (Meissnitzer, et al. 2009). The detection rate of SLUS was independent of the lesion size on MR imaging and malignant lesions were less likely to be detected on SLUS than benign lesions (Candelaria and Fornage 2011).

A study (Park, et al. 2013) summarized how second-look ultrasound could detect breast lesions with a suspicious MR imaging appearance. First, it is required to predict the location of each lesion on US based on axial MR images which show the lesion's location relative to the mammary zones. Because 73% of mammographically detected cancers developed in a 1-cm-wide zone beneath the subcutaneous fat or anterior to the retromammary fat (Stacey-Clear, et al. 1993), on second-look sonography the operator should pay significant attention to areas surrounding the mammary fascia (Nakano, et al. 2012). Second, estimate the lesion's location according to the lesion-to-nipple distance. Third, make use of the surrounding tissues. The anterior and posterior mammary fascias and the adjacent tissue are important factors in correlating lesions on breast US. Fourth, based on the lesion size, shape and other characteristics are used to locate the lesion. As lesions are compressed in a vertical direction by the US probe, they tend to appear smaller, and round lesions tend to appear oval or elliptical compared with their appearance on MR images. Furthermore, co-existing lesions, including ductal extension, known fibroadenomas, cysts, scars, implants or a known index cancer, are good landmarks to differentiate between MR imaging and US.

The rationale of MRI image fusion with US-guided biopsy: Although SLUS enhancements in 70% (128/182) of unsuspected abnormalities were found on breast MRI, there were still 30% (54/182) which were sonographically occult, including 15% (8/54) cancer (Destounis, et al. 2009). It is widely accepted that MRI-guided biopsy is very useful (Griebsch, et al. 2006, Harms, et al. 1993, Kuhl, et al. 2000, Leach, et al. 2005, Nunes, et al. 1997, Weinreb and Newstead 1995). Results of MRI-guided methods for women at an average risk of cancer showed the SE and SP of 0.9 (0.57–0.99) and 0.99 (0.91–1.0) for automated biopsy and 1.0 (0.98–1.0) and 0.91(0.54–0.99) for vacuum-assisted biopsy, respectively, and for women at a high age risk of cancer the SE and SP are 0.90 (0.58–0.98) and 0.99 (0.92–1.0) for automated biopsy and 0.99 (0.98–1.0) and 0.92(0.61–0.99) for

vacuum-assisted, biopsy respectively (Dahabreh, et al. 2014). Sakamoto (Sakamoto, et al. 2010) considered that the higher falsenegative rate of US-VAB for MRI-detected lesions (26%) than for US detected lesions (7.4%) was caused by the difficulties in MRI-US correlation, and which indicates the need for MRI-guided biopsy.

MRI-guided biopsy is time- and cost-consuming, and the prone patient position increases their inconvenience and tension. For MRI-guided biopsy, a patient in the prone position is repeatedly transferred in and out of the unit in order to estimate the location of the lesion and confirm placement of the needle. As the lesion might move during the needle insertion, and the position of the biopsy needle cannot be displayed in real-time images, there might be error in sampling. Several robotic systems and actuators for MRI-guided applications are being developed. US-guided biopsy has considerable advantages over MR imaging–guided biopsy, including its accessibility, efficacy, real-time visualization of lesions and biopsied tissue, cost-effectiveness, and less stress and discomfort for the patient. Therefore, it is necessary to construct a system combining MRI imaging and a sonogram.

Combined real-time ultrasound and MRI navigation system (RtMR-US): With real-time Volume Navigation development, US examinations and US guided biopsies can be navigated using other imaging data. The structures invisible to US but visible to other imaging modalities can be operated using US-guided biopsy navigated by the other modality. The number of identifiable lesions seen on US and the accuracy of image-guided intervention are increased if co-registration was made.

Technique and principle: Because Information regarding fusion medical imaging was obtained using different imaging modalities, spatial registration is required to assure that each pixel from different data sets represents approximately the same volume. Hipwell (Hipwell, et al. 2016) reviewed the current research and relevant publications of breast biomechanics modeling, breast image registration, and simulation algorithms. Image registration and data redistribution require manually co-registering a series of key points based on anatomic structures and the location of a lesion or fiducial markers before computer processing. The registration algorithm requires the measurement and identification of the orientation of the coordinate's marker and transformation matrix in order to assure that the same point is marked on each image. The image fusion could be maintained in static and real-time. In static fusion, the 3D image data of two modalities were stored in one workstation; after co-registering the data of two modalities, the structure and lesion of each modality could be easily compared and evaluated on the fusion image. In real-time fusion, the data of MRI/PET/CT is saved in the US-guided navigation systems, and the MRI/PET/CT image of the aligned plane will be displayed in real time during an ultrasound examination and intervention. Patient movement and the difference of their position between each examination can lead to distortion and affect the entire image fusion. Real-time fusion of ultrasound with MRI or CT is commercially available in brain, breast, liver, prostate, kidney, musculoskeletal, endoscopic ultrasound, and interventional modalities (Ewertsen, et al. 2013).

The real–time, Ultrasound–guided, MRI navigation system enables simultaneous display of the same site of both imaging modalities side-by-side or superimposed. Breast MRI should

be performed with the patient in the same position as on ultrasound, i.e. the supine position with the arm raised. As skin maker, before MRI, three vitamin E soft-gel capsules could be fixed on 3,9,and 12 o'clock on the nipple (Pons, et al. 2014). After MRI, the skin markers are covered with a transparent dressing to replace the soft gel capsules. The MRI data in the format of digital imaging and communications in medicine (DICOM) was transferred to the ultrasound–guided, virtual navigation systems. The small sensor installed in the ultrasonic probe and electromagnetic tracking system, i.e. electromagnetic transmitter, provided information regarding the position and orientation for the fusion system. Figure 13 shows the US and RtMR-US system. The rigid transformation matrix allows probe movement and makes rotations arbitrary. As the patient is being scanned using sonography, the navigation system identifies the position and motion of the probe and simultaneously reconstructs a corresponding slice of MRI from the previously imported volume data. The MRI of multi-planar reconstruction corresponding to the sonography image displayed real time at a rate exceeding 10 frames/s (Nakano, et al. 2009). When movement disturbs the coregistration image, adjusted function could be used for resynchronization.

Clinical research and results: A few studies have been published regarding the clinical applications of the ultrasound-MRI-guided system for breast biopsy. Preliminary experience by Fausto and co-workers (Fausto, et al. 2012) showed that the volume navigation technique of combined US-MR of the breast in normal breast tissue appears to be feasible, accurate, and reproducible. Live US images combined with contrast-enhanced MR is able to show the morphology of the glandular tissue with specific anatomic details (Figure 14). Pons (Pons, et al. 2014) showed the diagnostic performance of RtMR-US for breast lesions and axillary lymph nodes found on MRI and not on second-look US. The detection rate of the navigation technique (90.7%) was higher than that of conventional US (43%). The diagnostic performance of the MR-US navigation technique for identifying malignant nodules among overall lesions and axillary lymph nodes was: sensitivity 96.3% and 100%; specificity 18.8% and 30.7%; positive predictive value 66.7% and 43.7%; and negative predictive value 75% and 100%. Nakano conducted a series of studies using real-time virtual sonography (RVS) for detecting breast cancer. In 2009 Nakano (Nakano, et al. 2009) showed the sensitivity of RVS combined with MRI to be 98% for breast tumors and 83% for incidentally enhancing lesions. In 2012, Nakano (Nakano, et al. 2012) found that 90% of MRI-detected lesions were identified with second- look sonography using RVS, while the detection rate of MRI-detected lesions using the conventional B-mode was limited to 30%. In his research of 2012 (Nakano, et al. 2012), he showed that RVS combined with MRI can identify many more occult lesions than conventional B-mode, and the sonographic size of the lesions detected by RVS alone was significantly smaller than that of lesions detected by conventional B-mode. Figure 15 shows RVS detecting the MRI-enhancing lesions. The overall mean positioning error from the actual sonographic position to the expected MRI position in the three planes was 7.7 mm, 6.9mm, and 2.8mm for the x-, y-, and z-planes, respectively. In 2014, Nakano showed the result (Nakano, et al. 2014) that RVS coordinating the present US image with the past US image is a reproducible, operator-independent technique for comparison of US images of BI-RADS category 3 mass lesions obtained at different time points.

Hybrid ultrasound/MRI fusion system: In addition to the navigation systems, there are a few studies exploring other methods for the coregistration of breast MRI and US. In 2003, Piron (Piron, et al. 2003) developed a hybrid biopsy system combining ultrasound and MRI. In this system, the breast was immobilized between lateral and medial compression plates, each supporting a breast MR coil. After pre-biopsy MRI, the MR coils were removed. The lateral fenestrated compression plate is for the biopsy plug which guides the needle at a defined position and angle. The medial compression plate has acoustical membrane for the US probe. The parameters for the appropriate transducer position and biopsy-needle trajectory were calculated based on the result of MRI to select the proper needle approach to the lesion. The lesion detected by MRI is identical to the US image. Piron performed an experiment with breast tissue mimicking the phantom and in which the average accuracy score for MRI/US guidance and MRI guidance alone were 9.6 and 7.4, the average needle correction measured for all MRI/US guidance trail was calculated to be 3.7mm, and then the hybrid system were completely extended to clinic for two patients in the prone position. The limit is for the tissue near the chest wall. In 2008, their team (Causer, et al. 2008) subsequently presented the accuracy of the same MRI–sonography coregistration system in vivo: the mean lesion size correlated well on MRI (11.4 mm; range, 6–28 mm) compared with that of sonography (10.3 mm; range, 6–28 mm). All three masses were determined to be invasive ductal carcinoma on histopathology. The mean error measurements in the three planes were as follows: 2.5 mm for the x-plane, 1.1 mm for the y-plane, and 2.6 mm for the z-plane. This system is currently being developed and is not yet commercially available. Other novel phantoms of the hybrid breast biopsy system combining both modalities with negligible broadband noise and minimal periodic RF noise have been studied (Tang, et al. 2008).

PET, PET-CT, PEM and CT for breast cancer biopsy and navigating ultrasound-guided biopsy

Positron Emission Mammography (PEM) has a high PPV of 0.88 and depicts some breast malignancies not seen on mammograms and/or US images (Berg, et al. 2006). High-resolution, PEM-guided biopsy has been performed for the sampling of PET-depicted breast lesions in several, published studies (Argus and Mahoney 2014, Kalinyak, et al. 2011). Recent studies attempted to develop methods with low level of activities of 18 F-FDG, and nearly real-time visualization showed that PEM could detect a low level of activity of 18 F-FDG in order to decrease the radiation dose (Argus and Mahoney 2014, Choudhery and Seiler 2015). A system of nearly real-time visualization of lesion displacement simulation during the procedure of PEM–guided, breast biopsy has been developed (Lu, et al. 2008).

Combining 18F-FDG PET/CT with US or MRI could improve the diagnostic performance for the detection of axillary-node metastasis compared to 18F-FDG PET/CT alone (An, et al. 2014). One study has reported the fusion of US-guided navigation with PET/CT to facilitate identification and excision of suspicious axillary lymph node (Futamura, et al. 2013).

In addition, a pilot study (Kousaka, et al. 2014) that detected breast lesions with computed tomography (CT) coordinated real-time sonography images suggested that targeted sonography using real-time virtual sonography is a useful technique for identifying

incidentally detected breast lesions on chest CT. Yamamoto (Yamamoto, et al. 2010) showed that US guided by RVS was able to detect all of the same sentinel lymph nodes visualized by CT in seven of the 60 patients.

Ultrasound/mammography combining guided biopsy

Surry (Surry, et al. 2007) proposed an alternative dual modality system that combines stereotactic mammography (SM) imaging for position information with real-time 3D US imaging for guidance information. The breast probe of the 3D US-guided biopsy system is mounted on an upright stereotactic mammography unit and with stereotactic mammography for pre-procedural imaging, real-time 2D and near real-time 3D US imaging for intraprocedural targeting and guidance, and 3D US imaging for verification of the needle penetrating the target immediately post-biopsy.

Summary

Integrated imaging modalities can potentially compensate the weakness of each other. First, ultrasound can reduce the interference of gas, calcification, and a variety of artifacts, together with the strength of flexible and realtime ultrasound imaging. Real-time image fusion with ultrasound can be accurately carried out to assess target lesions previously identified by another imaging modality, which may lead to many clinical applications. Second, ultrasound fusion imaging can guide biopsies to the lesions only visible by other modalities and can also avoid the disadvantage of other modalities that the needle and the lesion relationship cannot be tracked in real time. Third, an ultrasound fusion volume navigation technique can be used to scan the breast nodules requiring follow-up. The limitation of real-time image fusion of ultrasound with other modalities can include the registration accuracy. This error could be due to the dislocation or deformation of breast tissue and the registration algorithm. New algorithms have been developed for assessing organ motion induced by breathing and movement. More landmarks or a precise electromagnetic tracking system might improve the accuracy. In the following section, we will compare the accuracy of ultrasound with other imaging modalities for breast cancer diagnosis.

ACCURACY OF OTHER MODALITIES FOR BREAST CANCER DIAGNOSIS

Mammography and ultrasound for breast screening

Digital Mammography is an effective universal technique used to decrease the breast cancer mortality. Mammographic screening results in a highly significant decrease in breast cancer-specific mortality (Hofvind, et al. 2013). Long-term outcomes in 2,305,427, screened asymptomatic women (Cutler, et al. 2015) showed that the average cumulative incidence rate of the first case of invasive breast cancer increased by 0.20% each year; With 25 years of follow-up, 94.55% of the patients remained disease-free; and average of 0.23% of the postmenopausal women were diagnosed with a first case of invasive breast cancer each year. The specificity of a single mammographic examination was 94% to 97% (Humphrey, et al. 2002).

It was accepted that the relative risk (RR) for women older than 50 screened by mammography was dropped, although the sensitivity of mammography was substantially lower for women in their 40s than for older women. There was the greatest reduction of breast cancer deaths in the age group 60–69 years (33%), statistically significant effects in the age groups 55–59, 60–64, and 65–69 years, and a small effect in women 50–54 years (Nystrom, et al. 2002). Mammography could harms that over 10 years of biennial screening among 40-year-old women invited to be screened, approximately 400 women would have false-positive results on mammography and 100 women would undergo biopsy or fine-needle aspiration for each death from breast cancer prevented(Humphrey, et al. 2002). For a 40- or 50-year-old woman undergoing 10 years of annual mammograms, the cumulative risk of a false-positive result is about 61%(Pace and Keating 2014). We list relative risk of breast-cancer mortality with Mammography screening in Table 2. There have different suggestions about the starting age of screening. In November 2009 U.S. Preventive Services Task Force (USPSTF) recommended biennial screening mammography for women 50–74 years. For the women before the age of 50 years USPSTF recommended the decision to start regular, biennial screening mammography should be an individual one and take patient context into account, including the patient's values regarding specific benefits and harms. But both the American Cancer Society (ACS, Smith, Cokkinides, Brooks, Saslow, & Brawley, 2010) and the American College of Obstetricians and Gynecologists (ACOG,2011) recommend that mammography be initiated at age 40 and continued annually (Corbelli, et al. 2014).

Mammographic sensitivity for breast cancer declines significantly with increasing breast density (Kerlikowske, et al. 1996, Kolb, et al. 2002, Saarenmaa, et al. 2001). More than 40% of women between 25– 55 years have more than 50% parenchymal density (Stomper, et al. 1996), which partly explain the reason why sensitivity of mammogram was lower for 40s than older. In 577 new breast cancer patients breast parenchyma density in total breast was dense in 52% among women aged 26–49, 28% among women aged 50–59, and 9% among women age 60–92 (Saarenmaa, et al. 2001). The sensitivity of mammography is just 30% in women with extremely dense breasts (Mandelson, et al. 2000). The sensitivity and specificity of screening mammography examinations would increase with age, based the on BCSC data through 2009(Consortium 2014). Moreover, increased mammographic breast density is a moderately independent risk factor for breast cancer in older women. The odds ratio for developing breast cancer for the most dense compared with the least dense breast tissue categories ranges from 1.8 to 6.0 (Harvey and Bovbjerg 2004).

Ultrasound is an extensively used breast imaging modality in the clinical setting and it is relatively inexpensive and with a high degree of patient acceptability. Although in women over age 50, mammography was more sensitive for detecting breast cancer than US (Sensitivity of mammography 0.95, Sensitivity of US 0.85) (Saarenmaa, et al. 2001), in women 45 years old or younger the sensitivity of sonography was 13.2% greater than that of mammography (Houssami, et al. 2003). US has been shown to have great value as a complementary examination to mammography, especially in younger age patients groups, and with mammography-negative and dense breast parenchyma (Corsetti, et al. 2008, Crystal, et al. 2003) (Saarenmaa, et al. 2001) and with tumors larger than 2 cm (Skaane, et al. 1999). The combined use of mammography and US has been reported to be an effective

tool in the detection of breast cancer. For example, the combination resulted in a sensitivity and specificity of 92.0% and 97.7%, respectively, in an observational follow-up study (Duijm, et al. 1997). The diagnostic accuracy for mammography was reported to increase from 0.78 to 0.91 for mammography plus US (Berg, et al. 2008). The addition of US for screening significantly increased the detection of small tumors and improved the breast cancer detection at a lower stage (Kolb, et al. 2002).

MRI for breast cancer diagnosis

MRI has a number of morphological sequences to evaluate breast tissue density and morphological changes and to assess the condition of the skin, armpits, and the edge of the pectoral muscle. Breast MRI has the ability to detect malignancy that is clinically and mammographically occult and to provide a high negative predictive value (NPV) that may help to safely exclude a diagnosis of malignancy (Moy, et al. 2009). Table 3 shows a comparison of the diagnostic performance of multimodality for breast cancer diagnosis. MRI might find a new lesion in breast cancer patients who have been diagnosed. It was reported that MRI made 69 additional findings in 99 patients of breast cancer, among them 51 findings were true-positives, including 16 larger single lesions, 18 cases of multifocality, seven cases of multicentricity, three cases of contralateral lesions, and five cases of lymph-node involvement(Mameri, et al. 2008). An additional detection for MRI was estimated at 16% in meta-analysis (Houssami and Hayes 2009).

Many studies have reported that breast MRI is a promising method for screening young women at high riskfor breast cancer (Kuhl, et al. 2000) (Kriege, et al. 2004) (Tilanus-Linthorst, et al. 2000) (Warner, et al. 2001) (Kuhl, et al. 2005, Sardanelli, et al. 2007, Warner, et al. 2004). Kuhl et al. (Kuhl, et al. 2005) reported that the SE of MRI (90.7%) significantly higher than that of mammography (39.5%) and ultrasound (36.2%) in the carriers of a breast cancer susceptibility gene, while the SP was equivalent. Diagnosis of intraductal and invasive breast cancer in familial or hereditary cancer is achieved with a significantly higher SE and at a more favorable stage using MRI surveillance than another modality (Kuhl, et al. 2005). In 2007, MRI was recommended by the American Cancer Society Guidelines for breast screening in patients with an approximately 20–25% or greater lifetime risk of breast cancer, including women with a strong family history of breast or ovarian cancer and women who were treated for Hodgkin's disease (Saslow, et al. 2007). However, the SP of MRI is not stable as 0.37–0.92 (Harms, et al. 1993, Leach, et al. 2005, Moy, et al. 2009) results in the need of further follow-up MRI and biopsy and as overall screening increased the costs, MRI is not the best choice as a breast cancer screening method. Annual screening with MRI and mammography improves metastasis-free survival in women with BRCA1 mutation or a familial predisposition (Saadatmand, et al. 2015). Contrast-enhanced MRI might be more a cost-effective screening modality than mammography as well as both strategies combined for women at high risk, particularly for the BRCA1 and BRCA2 subgroups (Griebsch, et al. 2006). MRI could help to improve the ability to diagnose ductal carcinoma in situ (DCIS) (Morris, et al. 2003). MR showed a higher SE than mammography for all tumor types and a higher SE than US for DCIS (Berg, et al. 2004), especially DCIS with a high nuclear grade (Kuhl, et al. 2007). Therefore, the indications for MRI are to diagnose tumor recurrence, screen high-risk patients, detect

primary tumors in patients with nodal metastases of unknown character, evaluate the response in patients treated with chemotherapy, and to analyze breast implants in order to rule out rupture (Tejerina Bernal, et al. 2012).

MRI does not currently seem to be effective in ruling out the need for biopsy in the assessment of sonographic BI-RADS 4 lesions (Sarica and Uluc 2014). When only ultrasonographic BI-RADS 4 lesions are considered, the SP of MRI was 56.7% (Sarica and Uluc 2014). In meta-analysis, the SP of contrast-enhanced MRI in patients with breast lesions is 0.72 (Peters, et al. 2008), and the pooled weighted SP of quantitative, diffusion-weighted (DW) MR imaging in patients with breast lesions was 0.84 (Chen, et al. 2010). Biopsy is still required in order to identify true positive lesions according to the results of breast MRI.

CT for breast cancer diagnosis

The value of CT for breast diseases has not yet been fully evaluated. In fact during routine chest CT examinations, the prevalence of breast cancers among incidental lesions detected varied from 24% to even 70%, therefore radiologists should pay attention to the breast (Son, et al. 2016). Furthermore, many scholars have been devoted to the study for dedicated breast CT (DBCT). In 2002, feasibility of cone-beam volume CT breast imaging technique was analyzed based on cone-beam X-ray projection volume imaging (Chen and Ning 2002). Since 2004, researchers have started to develop DBCT system capable of cone-beam CT and conducted clinical studies, contrastenhanced Breast CT (CEBCT) and DBCT comfort questionnaire (Lindfors, et al. 2008).

Prototype breast CT systems make use of flat panel detectors, which give rise to the half cone beam geometry (Lindfors, et al. 2010).The average glandular dose (AGD) from breast CT varied from 5 to 15 mGy (O'Connell, et al. 2014). The mean glandular dose from breast CT corresponds to the mean glandular dose from 4–5 mammography views and the mean number of views per breast during diagnostic mammography were 4.53 (Vedantham, et al. 2013). There was no statistical significance between the glandular dose from cone-beam CT and that from mammography (O'Connell, et al. 2010). Breast tissue coverage of CBCT was better in the lateral, medial and posterior, but inferior in the axilla and axillary tail compared with mammography (O'Connell, et al. 2010). Vedantham has investigated the system geometry with prone and upright breast CT positioning and achieved equivalent posterior breast coverage as mammograms (Vedantham, et al. 2013). The comparison between DBCT and other breast modalities are reported in a review paper (O'Connell, et al. 2014). In digital breast tomosynthesis the ability of separating the slices varies depending on object diameter and the arc span, while in DBCT it is stable. The scan time of DBCT is 10 seconds and a bilateral CEBCT can be done within a few minutes. Single injection of contrast media can complete bilateral CEBCT (O'Connell, et al. 2014). DBCT usually scans one breast at a time, and needs patient reposition for bilateral exam. DBCT can detect all masses detected by mammography (O'Connell, et al. 2010) and significantly improve visualization in shape and margin of suspicious masses (Kuzmiak, et al. 2016), especially in patients with dense breast tissue (Wienbeck, et al. 2017), but detection of calcifications is controversial. Kuzmiak has shown the reader confidence for calcification with CBCT was reduced

(Kuzmiak, et al. 2016). In another study cone-beam breast computed tomography (CBBCT) accurately distinguished DCIS from benign causes of microcalcifications when compared with mammography (Wienbeck, et al. 2017)

A prospective study of pathologically confirmed 110 lesions showed that DBCT provided high-quality images of the breast and could help radiologists to diagnose malignant breast lesions, as compared with ultrasound and digital mammography (He, et al. 2016). In a recent study, DBCT was used to identify breast lesion and was compared with BI-RADS Mammography Atlas, the estimated overall sensitivity of the readers was 0.969, and the specificity was 0.529 (Jung, et al. 2017).

CEBCT could increase conspicuity of benign and malignant mass and it has potential for evaluating extent of disease and for monitoring chemotherapy (O'Connell, et al. 2014). As for the molecular and pathological type, Ki-67, ER, PR, and HER2 did not correlate with CT density of breast cancer. Tubular carcinoma tended to have a higher CT density in comparison to other subtypes of breast carcinomas (Wienbeck, et al. 2017).

PET, PET-CT, and PEM for breast cancer diagnosis

PET, one of the most frequently utilized tumor imaging modalities, quantitatively presents metabolic activity to reflect lesion characterization and to contribute to treatment planning. FDG PET imaging screens the entire patient for local recurrence, lymph-node metastases, and distant metastases, and at a relatively low detection rate of bone metastases (Lind, et al. 2004). PET scans provide a high positive-predictive value (96.6%) for patients suggestive of primary breast cancer (Avril, et al. 2000). Partial volume effects and varying metabolic activity, depending on the tumor type, seem to represent the most significant limitations for the routine diagnostic application of PET (Avril, et al. 2000). Breast cancers with higher SUV can be overestimated due to the overflow effect, while small cancers with lower SUV can be underestimated due to the partial volume effect. According to the breast tumor size, the accuracy of FDG PET (43.5%) was significantly lower than that of MRI (91%) (Uematsu, et al. 2009). Tumor histology may influence the usefulness of 18F-FDG PET/CT for systemic staging of patients with breast cancer. For instance, invasive lobular carcinoma would have a greater possibility of non-FDG-avid sclerotic osseous metastases than invasive ductal carcinoma (Dashevsky, et al. 2015). FDG-PET had a very low SE (33.33%) for invasive breast cancers even though it had high SP (93.42 %)

Positron emission tomography–computed tomography (PET-CT) allows the merging of morphological and functional images. The rather low SP of FDG PET for breast cancer can be improved by utilizing combined anatomical-molecular imaging techniques, such as PET/CT tomography(Lind, et al. 2004). Whole-body PET-CT is extremely useful in tumor staging at a distance; especially in advanced stage breast cancer cases and also has a role in locoregional lymph-node staging. Distant metastases were detected with 18F-FDG PET/CT in 100% (Heusner, et al. 2008). Riedl (Riedl, et al. 2014) suggested that PET/CT might be valuable in younger patients with stage IIB and III disease. The patient-based SE and SP of FDG PET/CT were 96% and 89%, respectively (Lind, et al. 2004).While the SE was similar to that in their previous study using FDG PET alone, the SP was significantly higher for PET/CT (Lind, et al. 2004). The other research studies report that the SE of PET/CT and US

for the diagnosis of breast cancer were 86% and 91%, respectively (He, et al. 2015). As PET/CT is very expensive and not superior to US for detecting primary breast cancer, therefore it cannot be recommended as the primary diagnostic procedure for early breast cancer (He, et al. 2015).

Positron emission mammography (PEM) is a high spatial resolution tomographic method for molecular imaging of positron-emitting isotopes. PEM was approved by the US Food and Drug Administration and has been introduced into clinical use as a diagnostic adjunct to mammography and breast ultrasonography. PEM detected more newly diagnosed breast tumors (92 %) than whole-body PET (56 %) or PET/CT (87%). (Kalinyak, et al. 2014) PEM and MR imaging had comparable breast-level SE (Kalles, et al. 2013), i.e. 80.5% and 80.7%, for all of breast malignancies, 51% and 60% for additional foci of tumor, respectively, (Berg, et al. 2011), in addition to the SP of PEM (91.2%), is higher than that for MR imaging 86.3% (Berg, et al. 2011).

Summary

Imaging modalities for detection of breast cancers have been continuously improved and upgraded with new techniques, leading to improved diagnostic performance and reduced false negative rate. In the era of personalized medicine, doctors' knowledge regarding various imaging technologies will help to select the most accurate diagnostic method suitable for breast cancer diagnosis. In addition to breast cancer biopsy and diagnosis, ultrasound has also been utilized for detecting lymph node metastasis as discussed in the following section.

ULTRASOUND AND OTHER MODALITIES FOR LYMPH-NODE DIAGNOSIS

Axillary lymph-node metastasis is closely related to the prognosis of breast cancer. However, determination of the status of lymph nodes cannot rely on clinical examination as many lymph-node metastases are not palpable. Ultrasonography is used to detect axillary lymph nodes, depending on their size, shape, cortical thickness, and echo in order to determine their status [7–9]. A node is confirmed to be abnormal based on the following ultrasound features: oval to rounded shape; hypoechoic appearance with the absence of fatty hilum; eccentric cortical hypertrophy; lobulation; and a diameter larger than 4–5mm. Pre-operative, axillary ultrasound is crucial for the staging and management of breast cancer in many clinical institutions (Gentilini and Veronesi 2012), and it can detect some of the metastases and reduce the number of false–negatives biopsies. In addition, MRI and FDG PET CT can act as selected candidates for predicting SLNB. We present the major published results regarding the diagnostic performance of difference imaging modalities for detecting breast lymph nodes (Table 4). FDG PET imaging screens patients with breast cancer for lymph-node metastases with a reported average SE (47.7%-92.2%) and SP (81.6%-92%), respectively. The diagnostic accuracy of PET/CT is correlated with the ALN size (Zhang, et al. 2014). Some studies have shown that the presence of internal mammary (IM) lymph-node metastasis is a useful prognostic indicator and that IM metastasis has been associated with higher rates of distant disease and lower overall patient survival rates (Cody and Urban

1995, Sugg, et al. 2000). PET has excellent performance for evaluating internal mammary lymph-node metastasis (SE = 0.85, SP =0.90, Accuracy =0.88) (Eubank, et al. 2001).

Sentinel lymph nodes (SLN) can be an accurate predictor of the status of the axillary nodes. Currently, sentinel lymph-node biopsy (SLNB) has become the standard alternative for axillary lymph-node dissection (ALND) for assessing axillary lymph-node stages and reducing postoperative complications in breast cancer patients (Naik, et al. 2004) (Mansel, et al. 2006). The National Surgical Adjuvant Breast and Bowel Project (NSABP) trial B-32 showed that overall patient survival, disease-free survival, and regional control were statistically equivalent between the SLN resection plus ALND group and the SLN resection alone group, and which explained that when the SLN is negative, SLN surgery alone with no further ALND is an appropriate, safe, and effective therapy for breast cancer patients with clinically negative lymph nodes (Krag, et al. 2010), even in small breast cancers with a diameter   2 cm (Veronesi, et al. 2003). For comparison of the axillary lymph-node extent between patients with positive nodes determined using ultrasound-guided needle biopsy (USNB) and positive nodes in SLNB, Boone (Boone, et al. 2015) demonstrated that breast cancer patients with a positive node detected on ultrasound-guided biopsy have a significantly greater possibility of axillary disease than patients with a positive sentinel lymph node. In any case, ultrasound-detected abnormal lymph nodes can be histologically confirmed by ultrasound-guided biopsy in order to reduce unnecessary sentinel lymph-node biopsy (SLNB) or even axillary lymph-node dissection (ALND) and maximally invasive radical resection (Moorman, et al. 2014).

As reported in the literature, 3D multi-detector-row CT–lymphography using iopamidol is a reliable method for the preoperative detection of SLNs and the prediction of SLN metastasis in breast cancer patients (Suga, et al. 2005). Yamamoto (Yamamoto, et al. 2010) use a 3D CT lymphography system-guided US to identify SLNs in breast cancer patients. All of the seven SLNs visualized by 3D CT-LG can be detected using the RVS system and four of seven were confirmed as metastasis. The virtual multiplanar reconstruction image of the SLN was displayed in synchronization with the US image. SLN metastases were assessed by the shape and visibility of the hilum. Yamamoto also reported that if the cortical thickness of the SLN is great than 2.5 mm, the detection accuracy of the real-time, virtual sonography systems could increase (Yamamoto, et al. 2012).

In several other studies (Mi Cheng-rong 2010, Wang, et al. 2009, Zhong Li-yao 2007), ultrasound contrast agents were injected subcutaneously surrounding breast lesion, and then SLN enhancement degree and enhancement pattern were observed before methylene blue staining and resection. Because of hypoperfusion of pathological identified metastatic, SLN have showed asymmetrical enhanced and a few are low degree enhanced. A large validation and quantitative method needs to be developed in order to differential metastases SLN confidently.

CONCLUSION AND FUTURE DIRECTIONS

In this review we provide a broad overview of ultrasound imaging techniques for breast cancer detection and ultrasound-guided biopsy and fusion with other modalities. These

techniques are of great importance in diagnosing breast lesions as benign or malignant and can further improve early breast-cancer detection. This review could serve as a tutorial for medical residents, junior radiologists, and researchers who are interested in breast- cancer imaging and detection. The limitation of this review is that we haven't addressed every aspect of ultrasound imaging for breast cancer in detail.

For breast cancer screening, ultrasound has been applied as an adjunct imaging tool for mammography. Handheld ultrasound for the whole breast is time-consuming. A large pendulous breast increases the difficulties of ultrasound exams. Although more breast lesions could be found, most of them are benign (Lashkari, et al. 2016), which increases the false-positive rate of breast cancer screening and increases biopsy recommendations in screening (Health Quality Ontario 2016). For breast cancer detection and diagnosis, among many new techniques, breast ultrasound presents quite useful and comprehensive information, including lymph node in the axilla, between the pectoral muscle, the subclavian region, the neck, and the medial thoracic chain. The flexibility of ultrasound is superior to other modalities and this advantage is prominent on biopsy, follow-up and fusion with other modalities. Techniques for detecting breast tumor morphology and metabolic activities are constantly improving. Therefore, it is necessary to integrate new technologies for breast-cancer diagnosis and treatment services. CAD makes ultrasonic quantitative analysis possible and provides reliable and operator-independent technique for breast ultrasound diagnosis. In the future, effective CAD algorithms need to be validated widely in clinical practice. With the knowledge about the correlation between the sonographic features and pathological molecular markers and with the development of targeted contrast agents, breast ultrasound may provide molecular diagnosis in the future.

ACKNOWLEDGEMENTS

REFERENCES

U.S. Food and Drug Administration Medical devices: somo-v Automated Breast Ultrasound System (ABUS): P110006 [Internet]. Silver Spring, MD: U.S. Food and Drug Administration 2012 [cited 2014 Apr 10]. Available from: http://www.fda.gov/MedicalDevices/ProductsandMedicalProcedures/ DeviceApprovalsandClearances/Recently-ApprovedDevices/ucm320724.htm.

Ultrasound as an Adjunct to Mammography for Breast Cancer Screening: A Health Technology Assessment. Ontario health technology assessment series Health Quality Ontario 2016; 16:1–71.

Alvarez S, Aorbe E, Alcorta P, Lpez F, Alonso I, Corts J. Role of sonography in the diagnosis of axillary lymph node metastases in breast cancer: a systematic review. American Journal of Roentgenology 2006; 186:1342–48. [PubMed: 16632729]

An YS, Lee DH, Yoon JK, Lee SJ, Kim TH, Kang DK, Kim KS, Jung YS, Yim H. Diagnostic performance of 18F-FDG PET/CT, ultrasonography and MRI. Detection of axillary lymph node metastasis in breast cancer patients. Nuklearmedizin. Nuclear medicine 2014; 53:89–94. [PubMed: 24220324]

An YY, Kim SH, Kang BJ, Lee AW. Comparisons of Positron Emission Tomography/Computed Tomography and Ultrasound Imaging for Detection of Internal Mammary Lymph Node Metastases in Patients With Breast Cancer and Pathologic Correlation by Ultrasound-Guided Biopsy Procedures. Journal of ultrasound in medicine : official journal of the American Institute of Ultrasound in Medicine 2015; 34:1385–94. [PubMed: 26206824]

Argus A, Mahoney MC. Positron emission mammography: diagnostic imaging and biopsy on the same day. AJR. American journal of roentgenology 2014; 202:216–22. [PubMed: 24370147]

Athanasiou A, Tardivon A, Tanter M, Sigal-Zafrani B, Bercoff J, Deffieux T, Gennisson JL, Fink M, Neuenschwander S. Breast lesions: quantitative elastography with supersonic shear imaging--preliminary results. Radiology 2010; 256:297–303. [PubMed: 20505064]

Avril N, Rose CA, Schelling M, Dose J, Kuhn W, Bense S, Weber W, Ziegler S, Graeff H, Schwaiger M. Breast imaging with positron emission tomography and fluorine-18 fluorodeoxyglucose: use and limitations. Journal of clinical oncology : official journal of the American Society of Clinical Oncology 2000; 18:3495–502. [PubMed: 11032590]

Bai M, Du L, Gu J, Li F, Jia X. Virtual touch tissue quantification using acoustic radiation force impulse technology: initial clinical experience with solid breast masses. Journal of ultrasound in medicine : official journal of the American Institute of Ultrasound in Medicine 2012; 31:289–94. [PubMed: 22298873]

Balleyguier C, Ayadi S, Van Nguyen K, Vanel D, Dromain C, Sigal R. BIRADS classification in mammography. European journal of radiology 2007; 61:192–4. [PubMed: 17164080]

Balleyguier C, Opolon P, Mathieu MC, Athanasiou A, Garbay JR, Delaloge S, Dromain C. New potential and applications of contrast-enhanced ultrasound of the breast: Own investigations and review of the literature. European journal of radiology 2009; 69:14–23. [PubMed: 18977102]

Bamber J, Cosgrove D, Dietrich C, Fromageau J, Bojunga J, Calliada F, Cantisani V, Correas J, D'Onofrio M, Drakonaki E. EFSUMB guidelines and recommendations on the clinical use of ultrasound elastography. Part 1: Basic principles and technology. Ultraschall in der Medizin (Stuttgart, Germany : 1980) 2013; 34:169–84.

Barr RG. Sonographic breast elastography: a primer. Journal of ultrasound in medicine : official journal of the American Institute of Ultrasound in Medicine 2012; 31:773–83. [PubMed: 22535725]

Bastardis-Zakas K, Iatrakis G, Navrozoglou I, Peitsidis P, Salakos N, Malakassis P, Zervoudis S. Maximizing the benefits of screening mammography for women 40–49 years old. Clinical and experimental obstetrics & gynecology 2010; 37:278–82. [PubMed: 21355457]

Berg WA, Blume JD, Cormack JB, Mendelson EB, Lehrer D, Bohm-Velez M, Pisano ED, Jong RA, Evans WP, Morton MJ, Mahoney MC, Larsen LH, Barr RG, Farria DM, Marques HS, Boparai K. Combined screening with ultrasound and mammography vs mammography alone in women at elevated risk of breast cancer. Jama 2008; 299:2151–63. [PubMed: 18477782]

Berg WA, Cosgrove DO, Dore CJ, Schafer FK, Svensson WE, Hooley RJ, Ohlinger R, Mendelson EB, Balu-Maestro C, Locatelli M, Tourasse C, Cavanaugh BC, Juhan V, Stavros AT, Tardivon A, Gay J, Henry JP, Cohen-Bacrie C. Shear-wave elastography improves the specificity of breast US: the BE1 multinational study of 939 masses. Radiology 2012; 262:435–49. [PubMed: 22282182]

Berg WA, Gutierrez L, NessAiver MS, Carter WB, Bhargavan M, Lewis RS, Ioffe OB. Diagnostic accuracy of mammography, clinical examination, US, and MR imaging in preoperative assessment of breast cancer. Radiology 2004; 233:830–49. [PubMed: 15486214]

Berg WA, Madsen KS, Schilling K, Tartar M, Pisano ED, Larsen LH, Narayanan D, Ozonoff A, Miller JP, Kalinyak JE. Breast cancer: comparative effectiveness of positron emission mammography and MR imaging in presurgical planning for the ipsilateral breast. Radiology 2011; 258:59–72. [PubMed: 21076089]

Berg WA, Mendelson EB, Cosgrove DO, Doré CJ, Gay J, Henry J-P, Cohen-Bacrie C. Quantitative Maximum Shear-Wave Stiffness of Breast Masses as a Predictor of Histopathologic Severity. American Journal of Roentgenology 2015; 205:448–55. [PubMed: 26204299]

Berg WA, Weinberg IN, Narayanan D, Lobrano ME, Ross E, Amodei L, Tafra L, Adler LP, Uddo J, Stein W. High-Resolution Fluorodeoxyglucose Positron Emission Tomography with Compression ("Positron Emission Mammography") is Highly Accurate in Depicting Primary Breast Cancer. The breast journal 2006; 12:309–23. [PubMed: 16848840]

Bhatti PT, LeCarpentier GL, Roubidoux MA, Fowlkes JB, Helvie MA, Carson PL. Discrimination of sonographically detected breast masses using frequency shift color Doppler imaging in combination with age and gray scale criteria. Journal of ultrasound in medicine : official journal of the American Institute of Ultrasound in Medicine 2001; 20:343–50. [PubMed: 11316312]

Bluvol N, Kornecki A, Shaikh A, Del Rey Fernandez D, Taves DH, Fenster A. Freehand versus guided breast biopsy: comparison of accuracy, needle motion, and biopsy time in a tissue model. AJR. American journal of roentgenology 2009; 192:1720–5. [PubMed: 19457840]

Boone BA, Huynh C, Spangler ML, Sumkin J, Johnson R, McGuire KP, Soran A, Ahrendt GM. Axillary lymph node burden in invasive breast cancer: a comparison of the predictive value of ultrasoundguided needle biopsy and sentinel lymph node biopsy. Clinical breast cancer 2015; 15:e243–e48. [PubMed: 25922244]

Burbank F Stereotactic breast biopsy of atypical ductal hyperplasia and ductal carcinoma in situ lesions: improved accuracy with directional, vacuum-assisted biopsy. Radiology 1997; 202:843–7. [PubMed: 9051043]

Cai L, Wang X, Wang Y, Guo Y, Yu J, Wang Y. Robust phase-based texture descriptor for classification of breast ultrasound images. Biomedical engineering online 2015; 14:26. [PubMed: 25889570]

Calliada F, Campani R, Bottinelli O, Bozzini A, Sommaruga MG. Ultrasound contrast agents: basic principles. European journal of radiology 1998; 27 Suppl 2:S157–60. [PubMed: 9652516]

Candelaria R, Fornage BD. Second-look US examination of MR-detected breast lesions. Journal of clinical ultrasound : JCU 2011; 39:115–21. [PubMed: 21387324]

Caproni N, Marchisio F, Pecchi A, Canossi B, Battista R, D'Alimonte P, Torricelli P. Contrast-enhanced ultrasound in the characterisation of breast masses: utility of quantitative analysis in comparison with MRI. European radiology 2010; 20:1384–95. [PubMed: 20033178]

Carlsen JF, Ewertsen C, Lönn L, Nielsen MB. Strain elastography ultrasound: an overview with emphasis on breast cancer diagnosis. Diagnostics 2013; 3:117–25. [PubMed: 26835671]

Causer PA, Piron CA, Jong RA, Plewes DB. Preliminary in vivo validation of a dedicated breast MRI and sonographic coregistration imaging system. American Journal of Roentgenology 2008; 191:1203–07. [PubMed: 18806166]

Chae EY, Shin HJ, Kim HJ, Yoo H, Baek S, Cha JH, Kim HH. Diagnostic performance of automated breast ultrasound as a replacement for a hand-held second-look ultrasound for breast lesions detected initially on magnetic resonance imaging. Ultrasound in medicine & biology 2013; 39:2246–54. [PubMed: 24035627]

Chang RF, Hou YL, Lo CM, Huang CS, Chen JH, Kim WH, Chang JM, Bae MS, Moon WK. Quantitative analysis of breast echotexture patterns in automated breast ultrasound images. Medical physics 2015; 42:4566. [PubMed: 26233185]

Chen B, Ning R. Cone-beam volume CT breast imaging: feasibility study. Medical physics 2002; 29:755–70. [PubMed: 12033572]

Chen L, Chen Y, Diao X-H, Fang L, Pang Y, Cheng A-Q, Li W-P, Wang Y. Comparative study of automated breast 3-D ultrasound and handheld B-mode ultrasound for differentiation of benign and malignant breast masses. Ultrasound in medicine & biology 2013; 39:1735–42. [PubMed: 23849390]

Chen X, Li W-l, Zhang Y-l, Wu Q, Guo Y-m, Bai Z-l. Meta-analysis of quantitative diffusion-weighted MR imaging in the differential diagnosis of breast lesions. BMC cancer 2010; 10:1. [PubMed: 20047689]

Cheng H, Shan J, Ju W, Guo Y, Zhang L. Automated breast cancer detection and classification using ultrasound images: A survey. Pattern Recognition 2010; 43:299–317.

Choudhery S, Seiler S. Positron Emission Mammography Imaging with Low Activity Fluorodeoxyglucose and Novel Utilization in Core-needle Biopsy Sampling. World journal of nuclear medicine 2015; 14:63–5. [PubMed: 25709550]

Cody HS, 3rd, Urban JA. Internal mammary node status: a major prognosticator in axillary node-negative breast cancer. Annals of surgical oncology 1995; 2:32–7. [PubMed: 7834452]

Consortium BCS. Sensitivity and Specificity by Indication for Examination for 363,048 Diagnostic Mammography Examinations from 2004 – 2008 -- based on BCSC data through 2009. http://breastscreening.cancer.gov/statistics/benchmarks/diagnostic/2009/tableSensSpec.html Accessed December 16,2015.

Consortium BCS. Performance Measures for 1,838,372 Screening Mammography Examinations1 from 2004 to 2008 by Age -- based on BCSC data through 2009. http://breastscreening.cancer.gov/statistics/performance/screening/2009/perf_age.html 2014; Accessed December 16,2015.

Corbelli J, Borrero S, Bonnema R, McNamara M, Kraemer K, Rubio D, Karpov I, McNeil M. Physician adherence to U.S. Preventive Services Task Force mammography guidelines. Women's health issues : official publication of the Jacobs Institute of Women's Health 2014; 24:e313–9.

Corsetti V, Houssami N, Ferrari A, Ghirardi M, Bellarosa S, Angelini O, Bani C, Sardo P, Remida G, Galligioni E, Ciatto S. Breast screening with ultrasound in women with mammography-negative dense breasts: evidence on incremental cancer detection and false positives, and associated cost. European journal of cancer (Oxford, England : 1990) 2008; 44:539–44.

Crystal P, Strano SD, Shcharynski S, Koretz MJ. Using sonography to screen women with mammographically dense breasts. AJR. American journal of roentgenology 2003; 181:177–82. [PubMed: 12818853]

Curiel L, Chopra R, Hynynen K. Progress in multimodality imaging: truly simultaneous ultrasound and magnetic resonance imaging. Medical Imaging, IEEE Transactions on 2007; 26:1740–46.

Cutler W, Burki RE, Kolter JS, Chambliss C, Friedmann E. Breast Cancer Incidence in 2,305,427 Screened Asymptomatic Women: Long-Term Outcomes During Menopause [307]. Obstetrics & Gynecology 2015; 125:98S.

Dahabreh IJ, Wieland LS, Adam GP, Halladay C, Lau J, Trikalinos TA. Core Needle and Open Surgical Biopsy for Diagnosis of Breast Lesions: An Update to the 2009 Report. Rockville MD, 2014.

Dashevsky BZ, Goldman DA, Parsons M, Gönen M, Corben AD, Jochelson MS, Hudis CA, Morrow M, Ulaner GA. Appearance of untreated bone metastases from breast cancer on FDG PET/CT: importance of histologic subtype. European journal of nuclear medicine and molecular imaging 2015:1–8. [PubMed: 25319711]

del Cura JL, Elizagaray E, Zabala R, Legórburu A, Grande D. The use of unenhanced Doppler sonography in the evaluation of solid breast lesions. American Journal of Roentgenology 2005; 184:1788–94. [PubMed: 15908531]

Delle Chiaie L, Terinde R. Three-dimensional ultrasound-validated large-core needle biopsy: is it a reliable method for the histological assessment of breast lesions? Ultrasound in obstetrics & gynecology : the official journal of the International Society of Ultrasound in Obstetrics and Gynecology 2004; 23:393–7.

Dennison G, Anand R, Makar SH, Pain JA. A prospective study of the use of fine-needle aspiration cytology and core biopsy in the diagnosis of breast cancer. The breast journal 2003; 9:491–3. [PubMed: 14616944]

DeSantis C, Ma J, Bryan L, Jemal A. Breast cancer statistics, 2013. CA: a cancer journal for clinicians 2014; 64:52–62. [PubMed: 24114568]

Destounis S, Arieno A, Somerville PA, Seifert PJ, Murphy P, Morgan R, Skolny M, Hanson S, Young W. Community-based practice experience of unsuspected breast magnetic resonance imaging abnormalities evaluated with second-look sonography. Journal of ultrasound in medicine : official journal of the American Institute of Ultrasound in Medicine 2009; 28:1337–46.

Donna Fitzpatrick-Lewis NH, Ciliska Donna, Peirson Leslea, Gauld Mary, Yan Yun Liu McMaster University, Hamilton, Ontario, Canada Breast Cancer—Systematic Review.BREAST CANCER SCREENING. The Canadian Task Force on Preventive Health Care website 2011; http://canadiantaskforce.ca/ctfphc-guidelines/2011-breast-cancer/systematic-review/.

Duijm LE, Guit GL, Zaat JO, Koomen AR, Willebrand D. Sensitivity, specificity and predictive values of breast imaging in the detection of cancer. British journal of cancer 1997; 76:377–81. [PubMed: 9252206]

Duncan W, Kerr GR. The curability of breast cancer. British medical journal 1976; 2:781–3. [PubMed: 974608]

Eubank WB, Mankoff DA, Takasugi J, Vesselle H, Eary JF, Shanley TJ, Gralow JR, Charlop A, Ellis GK, Lindsley KL, Austin-Seymour MM, Funkhouser CP, Livingston RB. 18fluorodeoxyglucose positron emission tomography to detect mediastinal or internal mammary metastases in breast cancer. Journal of clinical oncology : official journal of the American Society of Clinical Oncology 2001; 19:3516–23. [PubMed: 11481358]

Evans A, Whelehan P, Thomson K, McLean D, Brauer K, Purdie C, Baker L, Jordan L, Rauchhaus P, Thompson A. Invasive breast cancer: relationship between shear-wave elastographic findings and histologic prognostic factors. Radiology 2012; 263:673–7. [PubMed: 22523322]

Evans A, Whelehan P, Thomson K, McLean D, Brauer K, Purdie C, Jordan L, Baker L, Thompson A. Quantitative shear wave ultrasound elastography: initial experience in solid breast masses. Breast cancer research : BCR 2010; 12:R104. [PubMed: 21122101]

Ewertsen C, S ftoiu A, Gruionu LG, Karstrup S, Nielsen MB. Real-time image fusion involving diagnostic ultrasound. American Journal of Roentgenology 2013; 200:W249–W55. [PubMed: 23436869]

Fausto A, Rizzatto G, Preziosa A, Gaburro L, Washburn MJ, Rubello D, Volterrani L. A new method to combine contrast-enhanced magnetic resonance imaging during live ultrasound of the breast using volume navigation technique: a study for evaluating feasibility, accuracy and reproducibility in healthy volunteers. European journal of radiology 2012; 81:e332–7. [PubMed: 22104088]

Fausto A, Rubello D, Carboni A, Mastellari P, Chondrogiannis S, Volterrani L. Clinical value of relative quantification ultrasound elastography in characterizing breast tumors. Biomedicine & Pharmacotherapy 2015; 75:88–92. [PubMed: 26463636]

Feng S, Lotz T, Chase JG, Hann CE. An image based vibration sensor for soft tissue modal analysis in a Digital Image Elasto Tomography (DIET) system. Conference proceedings: … Annual International Conference of the IEEE Engineering in Medicine and Biology Society. IEEE Engineering in Medicine and Biology Society. Annual Conference 2010; 2010:25–8.

Forsberg F, Goldberg BB, Merritt CR, Parker L, Maitino AJ, Palazzo JJ, Merton DA, Schultz SM, Needleman L. Diagnosing breast lesions with contrast-enhanced 3-dimensional power Doppler imaging. Journal of ultrasound in medicine 2004; 23:173–82. [PubMed: 14992354]

Futamura M, Morimitsu K, Nawa M, Kanematsu M, Gotoh N, Yoshida K. Novel navigation surgery using image fusion of PET/CT and sonography for axillary neoplasm: First experience. International journal of surgery case reports 2013; 4:719–22. [PubMed: 23811389]

Gentilini O, Veronesi U. Abandoning sentinel lymph node biopsy in early breast cancer? A new trial in progress at the European Institute of Oncology of Milan (SOUND: Sentinel node vs Observation after axillary UltraSouND). Breast (Edinburgh, Scotland) 2012; 21:678–81.

Gheonea IA, Stoica Z, Bondari S. Differential diagnosis of breast lesions using ultrasound elastography. The Indian journal of radiology & imaging 2011; 21:301–05. [PubMed: 22223946]

Giuseppetti GM, Martegani A, Di Cioccio B, Baldassarre S. Elastosonography in the diagnosis of the nodular breast lesions: preliminary report. La Radiologia medica 2005; 110:69–76. [PubMed: 16163141]

Goddi A, Bonardi M, Alessi S. Breast elastography: A literature review. Journal of ultrasound 2012; 15:192–8. [PubMed: 23449849]

Gokhale S Ultrasound characterization of breast masses. The Indian journal of radiology & imaging 2009; 19:242–7. [PubMed: 19881096]

Gomez W, Pereira WC, Infantosi AF. Analysis of co-occurence texture statistics as a function of gray-level quantization for classifying breast ultrasound. IEEE transactions on medical imaging 2012; 31:1889–99. [PubMed: 22759441]

Griebsch I, Brown J, Boggis C, Dixon A, Dixon M, Easton D, Eeles R, Evans DG, Gilbert FJ, Hawnaur J, Kessar P, Lakhani SR, Moss SM, Nerurkar A, Padhani AR, Pointon LJ, Potterton J, Thompson D, Turnbull LW, Walker LG, Warren R, Leach MO. Cost-effectiveness of screening with contrast enhanced magnetic resonance imaging vs X-ray mammography of women at a high familial risk of breast cancer. British journal of cancer 2006; 95:801–10. [PubMed: 17016484]

Hamashima C, Ohta K, Kasahara Y, Katayama T, Nakayama T, Honjo S, Ohnuki K. A meta-analysis of mammographic screening with and without clinical breast examination. Cancer science 2015; 106:812–18. [PubMed: 25959787]

Harms SE, Flamig DP, Hesley KL, Meiches MD, Jensen RA, Evans WP, Savino DA, Wells RV. MR imaging of the breast with rotating delivery of excitation off resonance: clinical experience with pathologic correlation. Radiology 1993; 187:493–501. [PubMed: 8475297]

Harvey JA, Bovbjerg VE. Quantitative assessment of mammographic breast density: relationship with breast cancer risk. Radiology 2004; 230:29–41. [PubMed: 14617762]

He N, Wu YP, Kong Y, Lv N, Huang ZM, Li S, Wang Y, Geng ZJ, Wu PH, Wei WD. The utility of breast cone-beam computed tomography, ultrasound, and digital mammography for detecting malignant breast tumors: A prospective study with 212 patients. European journal of radiology 2016; 85:392–403. [PubMed: 26781145]

He X, Shao M, Huo Y, Sun L, Ma C. A Comparative Study of 18F-FDG PET/CT and ultrasonography in the diagnosis of breast cancer and axillary lymph node metastasis. The quarterly journal of nuclear medicine and molecular imaging : official publication of the Italian Association of Nuclear Medicine (AIMN) [and] the International Association of Radiopharmacology (IAR), [and] Section of the So 2015.

Helbich TH, Rudas M, Haitel A, Kohlberger PD, Thurnher M, Gnant M, Wunderbaldinger P, Wolf G, Mostbeck GH. Evaluation of needle size for breast biopsy: comparison of 14-, 16-, and 18-gauge biopsy needles. AJR. American journal of roentgenology 1998; 171:59–63. [PubMed: 9648764]

Heusner TA, Kuemmel S, Hahn S, Koeninger A, Otterbach F, Hamami ME, Kimmig KR, Forsting M, Bockisch A, Antoch G. Diagnostic value of full-dose FDG PET/CT for axillary lymph node staging in breast cancer patients. European journal of nuclear medicine and molecular imaging 2009; 36:1543–50. [PubMed: 19415270]

Heusner TA, Kuemmel S, Umutlu L, Koeninger A, Freudenberg LS, Hauth EA, Kimmig KR, Forsting M, Bockisch A, Antoch G. Breast cancer staging in a single session: whole-body PET/CT mammography. Journal of nuclear medicine : official publication, Society of Nuclear Medicine 2008; 49:1215–22.

Hipwell JH, Vavourakis V, Han L, Mertzanidou T, Eiben B, Hawkes DJ. A review of biomechanically informed breast image registration. Physics in medicine and biology 2016; 61:R1–R31. [PubMed: 26733349]

Hofvind S, Ursin G, Tretli S, Sebuodegard S, Moller B. Breast cancer mortality in participants of the Norwegian Breast Cancer Screening Program. Cancer 2013; 119:3106–12. [PubMed: 23720226]

Houssami N, Hayes DF. Review of preoperative magnetic resonance imaging (MRI) in breast cancer: should MRI be performed on all women with newly diagnosed, early stage breast cancer? CA: a cancer journal for clinicians 2009; 59:290–302. [PubMed: 19679690]

Houssami N, Irwig L, Simpson JM, McKessar M, Blome S, Noakes J. Sydney Breast Imaging Accuracy Study: comparative sensitivity and specificity of mammography and sonography in young women with symptoms. American Journal of Roentgenology 2003; 180:935–40. [PubMed: 12646432]

Humphrey LL, Helfand M, Chan BK, Woolf SH. Breast cancer screening: a summary of the evidence for the US Preventive Services Task Force. Annals of internal medicine 2002; 137:347–60. [PubMed: 12204020]

Itoh A, Ueno E, Tohno E, Kamma H, Takahashi H, Shiina T, Yamakawa M, Matsumura T. Breast disease: clinical application of US elastography for diagnosis. Radiology 2006; 239:341–50. [PubMed: 16484352]

Jia W-R, Chai W-M, Tang L, Wang Y, Fei X-C, Han B-S, Chen M. Three-dimensional contrast enhanced ultrasound score and dynamic contrast-enhanced magnetic resonance imaging score in evaluating breast tumor angiogenesis: correlation with biological factors. European journal of radiology 2014; 83:1098–105.

Jiang Y-X, Liu H, Liu J-B, Zhu Q-L, Sun Q, Chang X-Y. Breast tumor size assessment: comparison of conventional ultrasound and contrast-enhanced ultrasound. Ultrasound in medicine & biology 2007; 33:1873–81. [PubMed: 17686569]

Jung EM, Jungius K-P, Rupp N, Gallegos M, Ritter G, Lenhart M, Clevert D-A, Kubale R. Contrast enhanced harmonic ultrasound for differentiating breast tumors-first results. Clinical hemorheology and microcirculation 2005; 33:109–20. [PubMed: 16151258]

Jung HK, Kuzmiak CM, Kim KW, Choi NM, Kim HJ, Langman EL, Yoon S, Steen D, Zeng D, Gao F. Potential Use of American College of Radiology BI-RADS Mammography Atlas for Reporting and Assessing Lesions Detected on Dedicated Breast CT Imaging: Preliminary Study. Academic radiology 2017.

Jung I, Kim MJ, Moon HJ, Yoon JH, Kim EK. Ultrasonography-guided 14-gauge core biopsy of the breast: results of 7 years of experience. Ultrasonography (Seoul, Korea) 2017.

Kalinyak JE, Berg WA, Schilling K, Madsen KS, Narayanan D, Tartar M. Breast cancer detection using high-resolution breast PET compared to whole-body PET or PET/CT. European journal of nuclear medicine and molecular imaging 2014; 41:260–75.

Kalinyak JE, Schilling K, Berg WA, Narayanan D, Mayberry JP, Rai R, Dupree EB, Shusterman DK, Gittleman MA, Luo W, Matthews CG. PET-guided breast biopsy. The breast journal 2011; 17:143–51. [PubMed: 21276128]

Kalles V, Zografos GC, Provatopoulou X, Koulocheri D, Gounaris A. The current status of positron emission mammography in breast cancer diagnosis. Breast cancer (Tokyo, Japan) 2013; 20:123–30.

Kaplan SS. Automated whole breast ultrasound. Radiologic clinics of North America 2014; 52:539–46. [PubMed: 24792655]

Kelly KM, Dean J, Lee SJ, Comulada WS. Breast cancer detection: radiologists' performance using mammography with and without automated whole-breast ultrasound. European radiology 2010; 20:2557–64. [PubMed: 20632009]

Kelly KM, Richwald GA. Automated whole-breast ultrasound: advancing the performance of breast cancer screening. Seminars in ultrasound, CT, and MR 2011; 32:273–80.

Keranen AK, Haapea M, Rissanen T. Ultrasonography as a Guiding Method in Breast Micro-Calcification Vacuum-Assisted Biopsies. Ultraschall in der Medizin (Stuttgart, Germany : 1980) 2015.

Kerlikowske K, Grady D, Barclay J, Sickles EA, Ernster V. Effect of age, breast density, and family history on the sensitivity of first screening mammography. Jama 1996; 276:33–8. [PubMed: 8667536]

Kim EA, Yoon KH, Lee YH, Kim HW, Juhng SK, Won JJ. Focal hepatic lesions: contrast-enhancement patterns at pulse-inversion harmonic US using a microbubble contrast agent. Korean journal of radiology 2003; 4:224–33. [PubMed: 14726639]

Kim YJ, Kim SH, Jeh SK, Choi JJ, Kang BJ, Song BJ. Gel pad application for automated breast sonography. Journal of ultrasound in medicine : official journal of the American Institute of Ultrasound in Medicine 2015; 34:713–9. [PubMed: 25792588]

Kisslo J, Firek B, Ota T, Kang DH, Fleishman CE, Stetten G, Li J, Ohazama CJ, Adams D, Landolfo C, Ryan T, von Ramm O. Real-time volumetric echocardiography: the technology and the possibilities. Echocardiography (Mount Kisco, N.Y.) 2000; 17:773–9.

Kolb TM, Lichy J, Newhouse JH. Comparison of the performance of screening mammography, physical examination, and breast US and evaluation of factors that influence them: an analysis of 27,825 patient evaluations. Radiology 2002; 225:165–75. [PubMed: 12355001]

Kousaka J, Nakano S, Ando T, Tetsuka R, Fujii K, Yoshida M, Shiomi-Mouri Y, Goto M, Imai Y, Imai T. Targeted sonography using an image fusion technique for evaluation of incidentally detected breast lesions on chest CT: a pilot study. Breast cancer (Tokyo, Japan) 2014:1–9.

Krag DN, Anderson SJ, Julian TB, Brown AM, Harlow SP, Costantino JP, Ashikaga T, Weaver DL, Mamounas EP, Jalovec LM, Frazier TG, Noyes RD, Robidoux A, Scarth HM, Wolmark N. Sentinel-lymph-node resection compared with conventional axillary-lymph-node dissection in clinically node-negative patients with breast cancer: overall survival findings from the NSABP B-32 randomised phase 3 trial. The Lancet. Oncology 2010; 11:927–33. [PubMed: 20863759]

Kriege M, Brekelmans CT, Boetes C, Besnard PE, Zonderland HM, Obdeijn IM, Manoliu RA, Kok T, Peterse H, Tilanus-Linthorst MM, Muller SH, Meijer S, Oosterwijk JC, Beex LV, Tollenaar RA, de Koning HJ, Rutgers EJ, Klijn JG. Efficacy of MRI and mammography for breast-cancer screening in women with a familial or genetic predisposition. The New England journal of medicine 2004; 351:427–37. [PubMed: 15282350]

Kuhl CK, Schmutzler RK, Leutner CC, Kempe A, Wardelmann E, Hocke A, Maringa M, Pfeifer U, Krebs D, Schild HH. Breast MR imaging screening in 192 women proved or suspected to be carriers of a breast cancer susceptibility gene: preliminary results. Radiology 2000; 215:267–79. [PubMed: 10751498]

Kuhl CK, Schrading S, Bieling HB, Wardelmann E, Leutner CC, Koenig R, Kuhn W, Schild HH. MRI for diagnosis of pure ductal carcinoma in situ: a prospective observational study. The Lancet 2007; 370:485–92.

Kuhl CK, Schrading S, Leutner CC, Morakkabati-Spitz N, Wardelmann E, Fimmers R, Kuhn W, Schild HH. Mammography, breast ultrasound, and magnetic resonance imaging for surveillance of women at high familial risk for breast cancer. Journal of clinical oncology : official journal of the American Society of Clinical Oncology 2005; 23:8469–76. [PubMed: 16293877]

Kuzmiak CM, Cole EB, Zeng D, Tuttle LA, Steed D, Pisano ED. Dedicated Three-dimensional Breast Computed Tomography: Lesion Characteristic Perception by Radiologists. Journal of clinical imaging science 2016; 6:14. [PubMed: 27195180]

Kvistad K, Rydland J, Smethurst H-B, Lundgren S, Fjøsne H, Haraldseth O. Axillary lymph node metastases in breast cancer: preoperative detection with dynamic contrast-enhanced MRI. European radiology 2000; 10:1464–71.

Lamuraglia M, Lassau N, Garbay JR, Mathieu MC, Rouzier R, Jaziri S, Roche A, Leclere J. Doppler US with perfusion software and contrast medium injection in the early evaluation of radiofrequency in breast cancer recurrences: a prospective phase II study. European journal of radiology 2005; 56:376–81. [PubMed: 16005593]

Lashkari AE, Pak F, Firouzmand M. Full Intelligent Cancer Classification of Thermal Breast Images to Assist Physician in Clinical Diagnostic Applications. Journal of Medical Signals and Sensors 2016; 6:12–24. [PubMed: 27014608]

Leach MO, Boggis CR, Dixon AK, Easton DF, Eeles RA, Evans DG, Gilbert FJ, Griebsch I, Hoff RJ, Kessar P, Lakhani SR, Moss SM, Nerurkar A, Padhani AR, Pointon LJ, Thompson D, Warren RM. Screening with magnetic resonance imaging and mammography of a UK population at high familial risk of breast cancer: a prospective multicentre cohort study (MARIBS). Lancet (London, England) 2005; 365:1769–78.

Lee H-J, Kim E-K, Kim MJ, Youk JH, Lee JY, Kang DR, Oh KK. Observer variability of Breast Imaging Reporting and Data System (BI-RADS) for breast ultrasound. European journal of radiology 2008; 65:293–98. [PubMed: 17531417]

Lee SH, Chang JM, Kim WH, Bae MS, Cho N, Yi A, Koo HR, Kim SJ, Kim JY, Moon WK. Differentiation of benign from malignant solid breast masses: comparison of two-dimensional and three-dimensional shear-wave elastography. European radiology 2013; 23:1015–26. [PubMed: 23085867]

Li D-D, Guo L-H, Xu H-X, Liu C, Xu J-M, Sun L-P, Wu J, Liu B-J, Liu L-N, Xu X-H. Acoustic radiation force impulse elastography for differentiation of malignant and benign breast lesions: a metaanalysis. International journal of clinical and experimental medicine 2015; 8:4753. [PubMed: 26131049]

Li N, Jiang YX, Zhu QL, Zhang J, Dai Q, Liu H, Yang Q, Wang HY, Lai XJ, Sun Q. Accuracy of an automated breast volume ultrasound system for assessment of the pre-operative extent of pure ductal carcinoma in situ: comparison with a conventional handheld ultrasound examination. Ultrasound in medicine & biology 2013; 39:2255–63. [PubMed: 24035630]

Liberman L, Feng TL, Dershaw DD, Morris EA, Abramson AF. US-guided core breast biopsy: use and cost-effectiveness. Radiology 1998; 208:717–23. [PubMed: 9722851]

Lind P, Igerc I, Beyer T, Reinprecht P, Hausegger K. Advantages and limitations of FDG PET in the follow-up of breast cancer. European journal of nuclear medicine and molecular imaging 2004; 31 Suppl 1:S125–34. [PubMed: 15085295]

Lindfors KK, Boone JM, Nelson TR, Yang K, Kwan AL, Miller DF. Dedicated breast CT: initial clinical experience. Radiology 2008; 246:725–33. [PubMed: 18195383]

Lindfors KK, Boone JM, Newell MS, D'Orsi CJ. DEDICATED BREAST CT: THE OPTIMAL CROSS SECTIONAL IMAGING SOLUTION? Radiologic clinics of North America 2010; 48:1043–54. [PubMed: 20868899]

Liu H, Tan T, van Zelst J, Mann R, Karssemeijer N, Platel B. Incorporating texture features in a computer-aided breast lesion diagnosis system for automated three-dimensional breast ultrasound. Journal of medical imaging (Bellingham, Wash.) 2014; 1:024501.

Lu X, Anashkin E, Matthews CG, Luo W. 2008 Real-time viewer for Positron Emission Mammography image-guided intervention. Nuclear Science Symposium Conference Record, 2008 NSS'08 IEEE: IEEE, 4814–19.

Mameri CS, Kemp C, Goldman SM, Sobral LA, Ajzen S. Impact of breast MRI on surgical treatment, axillary approach, and systemic therapy for breast cancer. The breast journal 2008; 14:236–44. [PubMed: 18476882]

Mandelson MT, Oestreicher N, Porter PL, White D, Finder CA, Taplin SH, White E. Breast density as a predictor of mammographic detection: comparison of interval- and screen-detected cancers. Journal of the National Cancer Institute 2000; 92:1081–7. [PubMed: 10880551]

Mansel RE, Fallowfield L, Kissin M, Goyal A, Newcombe RG, Dixon JM, Yiangou C, Horgan K, Bundred N, Monypenny I, England D, Sibbering M, Abdullah TI, Barr L, Chetty U, Sinnett DH, Fleissig A, Clarke D, Ell PJ. Randomized multicenter trial of sentinel node biopsy versus standard axillary treatment in operable breast cancer: the ALMANAC Trial. Journal of the National Cancer Institute 2006; 98:599–609. [PubMed: 16670385]

Meissnitzer M, Dershaw DD, Lee CH, Morris EA. Targeted ultrasound of the breast in women with abnormal MRI findings for whom biopsy has been recommended. AJR. American journal of roentgenology 2009; 193:1025–9. [PubMed: 19770325]

Meng W, Zhang G, Wu C, Wu G, Song Y, Lu Z. Preliminary results of acoustic radiation force impulse (ARFI) ultrasound imaging of breast lesions. Ultrasound in medicine & biology 2011; 37:1436–43. [PubMed: 21767903]

Mi Cheng-rong HY, Wen Wang. Proto-explore of ultrasound contrast agents injected subcutaneously for enhancement in sentinel lymph nodes of breast masses. Chinese Journal of Ultrasonography 2010; 19:970–3.

Miller AB, Wall C, Baines CJ, Sun P, To T, Narod SA. Twenty five year follow-up for breast cancer incidence and mortality of the Canadian National Breast Screening Study: randomised screening trial. Bmj 2014; 348.

Moon WK, Lo CM, Chang JM, Huang CS, Chen JH, Chang RF. Computer-aided classification of breast masses using speckle features of automated breast ultrasound images. Medical physics 2012; 39:6465–73. [PubMed: 23039681]

Moorman A, Bourez R, Heijmans H, Kouwenhoven E. Axillary ultrasonography in breast cancer patients helps in identifying patients preoperatively with limited disease of the axilla. Annals of surgical oncology 2014; 21:2904–10. [PubMed: 24715214]

Morris EA, Liberman L, Ballon DJ, Robson M, Abramson AF, Heerdt A, Dershaw DD. MRI of occult breast carcinoma in a high-risk population. AJR. American journal of roentgenology 2003; 181:619–26. [PubMed: 12933450]

Moss SM, Cuckle H, Evans A, Johns L, Waller M, Bobrow L. Effect of mammographic screening from age 40 years on breast cancer mortality at 10 years' follow-up: a randomised controlled trial. The Lancet 2006; 368:2053–60.

Moy L, Elias K, Patel V, Lee J, Babb JS, Toth HK, Mercado CL. Is breast MRI helpful in the evaluation of inconclusive mammographic findings? AJR. American journal of roentgenology 2009; 193:986–93. [PubMed: 19770320]

Nagarajan MB, Huber MB, Schlossbauer T, Leinsinger G, Krol A, Wismuller A. Classification of small lesions in dynamic breast MRI: Eliminating the need for precise lesion segmentation through spatio-temporal analysis of contrast enhancement over time. Machine vision and applications 2013; 24.

Naik AM, Fey J, Gemignani M, Heerdt A, Montgomery L, Petrek J, Port E, Sacchini V, Sclafani L, VanZee K, Wagman R, Borgen PI, Cody HS, 3rd, The risk of axillary relapse after sentinel lymph node biopsy for breast cancer is comparable with that of axillary lymph node dissection: a follow-up study of 4008 procedures. Annals of surgery 2004; 240:462–8; discussion 68–71. [PubMed: 15319717]

Nakano S, Ando T, Tetsuka R, Fujii K, Yoshida M, Kousaka J, Shiomi-Mouri Y, Imai T, Fukutomi T, Ishiguchi T, Arai O. Reproducible surveillance breast ultrasound using an image fusion technique in a short-interval follow-up for BI-RADS 3 lesions: a pilot study. Ultrasound in medicine & biology 2014; 40:1049–57. [PubMed: 24613559]

Nakano S, Kousaka J, Fujii K, Yorozuya K, Yoshida M, Mouri Y, Akizuki M, Tetsuka R, Ando T, Fukutomi T, Oshima Y, Kimura J, Ishiguchi T, Arai O. Impact of real-time virtual sonography, a coordinated sonography and MRI system that uses an image fusion technique, on the sonographic

evaluation of MRI-detected lesions of the breast in second-look sonography. Breast cancer research and treatment 2012; 134:1179–88. [PubMed: 22821400]

Nakano S, Yoshida M, Fujii K, Yorozuya K, Kousaka J, Mouri Y, Fukutomi T, Ohshima Y, Kimura J, Ishiguchi T. Real-time virtual sonography, a coordinated sonography and MRI system that uses magnetic navigation, improves the sonographic identification of enhancing lesions on breast MRI. Ultrasound in medicine & biology 2012; 38:42–9. [PubMed: 22137178]

Nakano S, Yoshida M, Fujii K, Yorozuya K, Mouri Y, Kousaka J, Fukutomi T, Kimura J, Ishiguchi T, Ohno K, Mizumoto T, Harao M. Fusion of MRI and sonography image for breast cancer evaluation using real-time virtual sonography with magnetic navigation: first experience. Japanese journal of clinical oncology 2009; 39:552–9. [PubMed: 19654132]

Nelson HD, Tyne K, Naik A, Bougatsos C, Chan BK, Humphrey L. Screening for breast cancer: an update for the US Preventive Services Task Force. Annals of internal medicine 2009; 151:727–37. [PubMed: 19920273]

Nunes LW, Schnall MD, Orel SG, Hochman MG, Langlotz CP, Reynolds CA, Torosian MH. Breast MR imaging: interpretation model. Radiology 1997; 202:833–41. [PubMed: 9051042]

Nystrom L, Andersson I, Bjurstam N, Frisell J, Nordenskjold B, Rutqvist LE. Long-term effects of mammography screening: updated overview of the Swedish randomised trials. Lancet (London, England) 2002; 359:909–19.

O'Connell A, Conover DL, Zhang Y, Seifert P, Logan-Young W, Lin CF, Sahler L, Ning R. Cone-beam CT for breast imaging: Radiation dose, breast coverage, and image quality. AJR. American journal of roentgenology 2010; 195:496–509. [PubMed: 20651210]

O'Connell AM, Karellas A, Vedantham S. The potential role of dedicated 3D breast CT as a diagnostic tool: review and early clinical examples. The breast journal 2014; 20:592–605. [PubMed: 25199995]

O'Connell AM, Irshad A, Nguyen MS. Breast Ultrasonography. Ultrasound Clinics 2013; 8:109–16.

Obdeijn I-MA, Brouwers-Kuyper EM, Tilanus-Linthorst MM, Wiggers T, Oudkerk M. MR imagingguided sonography followed by fine-needle aspiration cytology in occult carcinoma of the breast. American Journal of Roentgenology 2000; 174:1079–84. [PubMed: 10749254]

Pace LE, Keating NL. A systematic assessment of benefits and risks to guide breast cancer screening decisions. Jama 2014; 311:1327–35. [PubMed: 24691608]

Park VY, Kim MJ, Kim E-K, Moon HJ. Second-look US: how to find breast lesions with a suspicious MR imaging appearance. Radiographics : a review publication of the Radiological Society of North America, Inc 2013; 33:1361–75.

Parker SH, Jobe WE, Dennis MA, Stavros AT, Johnson KK, Yakes WF, Truell JE, Price JG, Kortz AB, Clark DG. US-guided automated large-core breast biopsy. Radiology 1993; 187:507–11. [PubMed: 8475299]

Peters NH, Borel Rinkes IH, Zuithoff NP, Mali WP, Moons KG, Peeters PH. Meta-analysis of MR imaging in the diagnosis of breast lesions. Radiology 2008; 246:116–24. [PubMed: 18024435]

Piron CA, Causer P, Jong R, Shumak R, Plewes DB. A hybrid breast biopsy system combining ultrasound and MRI. IEEE transactions on medical imaging 2003; 22:1100–10. [PubMed: 12956265]

Piscaglia F, Nolsøe C, Dietrich Ca, Cosgrove D, Gilja O, Bachmann Nielsen M, Albrecht T, Barozzi L, Bertolotto M, Catalano O. The EFSUMB Guidelines and Recommendations on the Clinical Practice of Contrast Enhanced Ultrasound (CEUS): update 2011 on non-hepatic applications. Ultraschall in der Medizin 2012; 33:33. [PubMed: 21874631]

Pons EP, Azcon FM, Casas MC, Meca SM, Espona JL. Real-time MRI navigated US: role in diagnosis and guided biopsy of incidental breast lesions and axillary lymph nodes detected on breast MRI but not on second look US. European journal of radiology 2014; 83:942–50. [PubMed: 24725672]

Radiology ACo. ACR BI-RADS Atlas Fifth Edition. http://www.acr.org/~/media/ACR/Documents/PDF/QualitySafety/Resources/BIRADS/Posters/BIRADS%20Poster_36x24in_F.pdf2015; Access December 16,2015.

Reinikainen HT, Rissanen TJ, Piippo UK, Paivansalo MJ. Contribution of ultrasonography and fineneedle aspiration cytology to the differential diagnosis of palpable solid breast lesions. Acta radiologica (Stockholm, Sweden : 1987) 1999; 40:383–9.

Ricci P, Cantisani V, Ballesio L, Pagliara E, Sallusti E, Drudi FM, Trippa F, Calascibetta F, Erturk SM, Modesti M, Passariello R. Benign and malignant breast lesions: efficacy of real time contrast-enhanced ultrasound vs. magnetic resonance imaging. Ultraschall in der Medizin (Stuttgart, Germany : 1980) 2007; 28:57–62.

Riedl CC, Slobod E, Jochelson M, Morrow M, Goldman DA, Gonen M, Weber WA, Ulaner GA. Retrospective analysis of 18F-FDG PET/CT for staging asymptomatic breast cancer patients younger than 40 years. Journal of Nuclear Medicine 2014; 55:1578–83. [PubMed: 25214641]

Roe SM, Mathews JA, Burns RP, Sumida MP, Craft P, Jr., Greer MS. Stereotactic and ultrasound core needle breast biopsy performed by surgeons. American journal of surgery 1997; 174:699–703; discussion 03–4. [PubMed: 9409600]

Saadatmand S, Obdeijn IM, Rutgers EJ, Oosterwijk JC, Tollenaar RA, Woldringh GH, Bergers E, Verhoef C, Heijnsdijk EA, Hooning MJ. Survival benefit in women with BRCA1 mutation or familial risk in the MRI screening study (MRISC). International Journal of Cancer 2015; 137:1729–38. [PubMed: 25820931]

Saarenmaa I, Salminen T, Geiger U, Heikkinen P, Hyvarinen S, Isola J, Kataja V, Kokko ML, Kokko R, Kumpulainen E, Karkkainen A, Pakkanen J, Peltonen P, Piironen A, Salo A, Talviala ML, Haka M. The effect of age and density of the breast on the sensitivity of breast cancer diagnostic by mammography and ultasonography. Breast cancer research and treatment 2001; 67:117–23. [PubMed: 11519860]

Sadigh G, Carlos RC, Neal CH, Dwamena BA. Ultrasonographic differentiation of malignant from benign breast lesions: a meta-analytic comparison of elasticity and BIRADS scoring. Breast cancer research and treatment 2012; 133:23–35. [PubMed: 22057974]

Sahiner B, Chan H-P, Roubidoux MA, Hadjiiski LM, Helvie MA, Paramagul C, Bailey J, Nees AV, Blane C. Malignant and Benign Breast Masses on 3D US Volumetric Images: Effect of Computer-aided Diagnosis on Radiologist Accuracy 1. Radiology 2007; 242:716–24. [PubMed: 17244717]

Sahiner B, Chan HP, Roubidoux MA, Hadjiiski LM, Helvie MA, Paramagul C, Bailey J, Nees AV, Blane C. Malignant and benign breast masses on 3D US volumetric images: effect of computer-aided diagnosis on radiologist accuracy. Radiology 2007; 242:716–24. [PubMed: 17244717]

Sakamoto N, Tozaki M, Higa K, Abe S, Ozaki S, Fukuma E. False-negative ultrasound-guided vacuum- assisted biopsy of the breast: difference with US-detected and MRI-detected lesions. Breast cancer (Tokyo, Japan) 2010; 17:110–7.

Samani A, Zubovits J, Plewes D. Elastic moduli of normal and pathological human breast tissues: an inversion-technique-based investigation of 169 samples. Physics in medicine and biology 2007; 52:1565–76. [PubMed: 17327649]

Sardanelli F, Podo F, D'Agnolo G, Verdecchia A, Santaquilani M, Musumeci R, Trecate G, Manoukian S, Morassut S, de Giacomi C, Federico M, Cortesi L, Corcione S, Cirillo S, Marra V, Cilotti A, Di Maggio C, Fausto A, Preda L, Zuiani C, Contegiacomo A, Orlacchio A, Calabrese M, Bonomo L, Di Cesare E, Tonutti M, Panizza P, Del Maschio A. Multicenter comparative multimodality surveillance of women at genetic-familial high risk for breast cancer (HIBCRIT study): interim results. Radiology 2007; 242:698–715. [PubMed: 17244718]

Sardanelli F, Podo F, Santoro F, Manoukian S, Bergonzi S, Trecate G, Vergnaghi D, Federico M, Cortesi L, Corcione S. Multicenter surveillance of women at high genetic breast cancer risk using mammography, ultrasonography, and contrast-enhanced magnetic resonance imaging (the high breast cancer risk italian 1 study): final results. Investigative radiology 2011; 46:94–105. [PubMed: 21139507]

Sarica O, Uluc F. Additional diagnostic value of MRI in patients with suspicious breast lesions based on ultrasound. The British Journal of Radiology 2014; 87:20140009. [PubMed: 24983629]

Saslow D, Boetes C, Burke W, Harms S, Leach MO, Lehman CD, Morris E, Pisano E, Schnall M, Sener S. American Cancer Society guidelines for breast screening with MRI as an adjunct to mammography. CA: a cancer journal for clinicians 2007; 57:75–89. [PubMed: 17392385]

Scaperrotta G, Ferranti C, Costa C, Mariani L, Marchesini M, Suman L, Folini C, Bergonzi S. Role of sonoelastography in non-palpable breast lesions. European radiology 2008; 18:2381–89. [PubMed: 18523780]

Shen S, Zhou Y, Xu Y, Zhang B, Duan X, Huang R, Li B, Shi Y, Shao Z, Liao H, Jiang J, Shen N, Zhang J, Yu C, Jiang H, Li S, Han S, Ma J, Sun Q. A multi-centre randomised trial comparing ultrasound vs mammography for screening breast cancer in high-risk Chinese women. British journal of cancer 2015; 112:998–1004. [PubMed: 25668012]

Shin HJ, Kim HH, Cha JH. Current status of automated breast ultrasonography. Ultrasonography (Seoul, Korea) 2015; 34:165.

Shin HJ, Kim HH, Cha JH. Current status of automated breast ultrasonography. Ultrasonography (Seoul, Korea) 2015; 34:165–72.

Shin HJ, Kim HH, Cha JH, Park JH, Lee KE, Kim JH. Automated ultrasound of the breast for diagnosis: interobserver agreement on lesion detection and characterization. AJR. American journal of roentgenology 2011; 197:747–54. [PubMed: 21862820]

Siegel RL, Miller KD, Jemal A. Cancer statistics, 2015. CA: a cancer journal for clinicians 2015; 65:5–29. [PubMed: 25559415]

Siegel RL, Miller KD, Jemal A. Cancer Statistics, 2017. CA: a cancer journal for clinicians 2017; 67:7–30. [PubMed: 28055103]

Sim Y, Vinnicombe S, Whelehan P, Thomson K, Evans A. Value of shear-wave elastography in the diagnosis of symptomatic invasive lobular breast cancer. Clinical radiology 2015; 70:604–09. [PubMed: 25770021]

Skaane P, Sager EM, Olsen JB, Abdelnoor M, Berger A, Wolff PA, Kullmann G. Diagnostic value of ultrasonography in patients with palpable mammographically noncalcified breast tumors. Acta radiologica (Stockholm, Sweden : 1987) 1999; 40:163–8.

Skaane P, Skjorten F. Ultrasonographic evaluation of invasive lobular carcinoma. Acta radiologica (Stockholm, Sweden : 1987) 1999; 40:369–75.

Skerl K, Vinnicombe S, Thomson K, McLean D, Giannotti E, Evans A. Anisotropy of Solid Breast Lesions in 2D Shear Wave Elastography is an Indicator of Malignancy. Academic radiology 2016; 23:53–61. [PubMed: 26564483]

Smith WL, Surry KJ, Mills GR, Downey DB, Fenster A. Three-dimensional ultrasound-guided core needle breast biopsy. Ultrasound in medicine & biology 2001; 27:1025–34. [PubMed: 11527588]

Son JH, Jung HK, Song JW, Baek HJ, Doo KW, Kim W, Kim YM, Kim WW, Lee JS, Cho EY. Incidentally detected breast lesions on chest CT with US correlation: a pictorial essay. Diagnostic and interventional radiology (Ankara, Turkey) 2016; 22:514–18.

Song SE, Seo BK, Cho KR, Woo OH, Son GS, Kim C, Cho SB, Kwon SS. Computer-aided detection (CAD) system for breast MRI in assessment of local tumor extent, nodal status, and multifocality of invasive breast cancers: preliminary study. Cancer imaging : the official publication of the International Cancer Imaging Society 2015; 15:1. [PubMed: 25888983]

Spick C, Baltzer PA. Diagnostic utility of second-look US for breast lesions identified at MR imaging: systematic review and meta-analysis. Radiology 2014; 273:401–9. [PubMed: 25119022]

Sridharan A, Eisenbrey JR, Machado P, Ojeda-Fournier H, Wilkes A, Sevrukov A, Mattrey RF, Wallace K, Chalek CL, Thomenius KE, Forsberg F. Quantitative analysis of vascular heterogeneity in breast lesions using contrast-enhanced 3-D harmonic and subharmonic ultrasound imaging. IEEE transactions on ultrasonics, ferroelectrics, and frequency control 2015; 62:502–10.

Stacey-Clear A, McCarthy KA, Hall DA, Pile-Spellman E, White G, Hulka CA, Whitman GJ, Halpern EF, Kopans DB. Mammographically detected breast cancer: location in women under 50 years old. Radiology 1993; 186:677–80. [PubMed: 8381550]

Stavros AT, Thickman D, Rapp CL, Dennis MA, Parker SH, Sisney GA. Solid breast nodules: use of sonography to distinguish between benign and malignant lesions. Radiology 1995; 196:123–34. [PubMed: 7784555]

Stoblen F, Landt S, Stelkens-Gebhardt R, Sehouli J, Rezai M, Kummel S. First evaluation of the diagnostic accuracy of an automated 3D ultrasound system in a breast screening setting. Anticancer research 2011; 31:2569–74. [PubMed: 21778306]
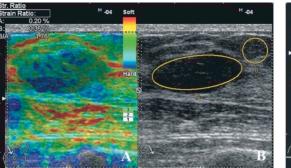
Stomper PC, D'Souza DJ, DiNitto PA, Arredondo MA. Analysis of parenchymal density on mammograms in 1353 women 25–79 years old. AJR. American journal of roentgenology 1996; 167:1261–5. [PubMed: 8911192]

Suga K, Yamamoto S, Tangoku A, Oka M, Kawakami Y, Matsunaga N. Breast sentinel lymph node navigation with three-dimensional interstitial multidetector-row computed tomographic lymphography. Investigative radiology 2005; 40:336–42. [PubMed: 15905719]

Sugg SL, Ferguson DJ, Posner MC, Heimann R. Should internal mammary nodes be sampled in the sentinel lymph node era? Annals of surgical oncology 2000; 7:188–92. [PubMed: 10791848]

Surry KJ, Mills GR, Bevan K, Downey DB, Fenster A. Stereotactic mammography imaging combined with 3D US imaging for image guided breast biopsy. Medical physics 2007; 34:4348–58. [PubMed: 18072500]

Tan T, Mordang J-J, van Zelst J, Grivegnée A, Gubern-Mérida A, Melendez J, Mann RM, Zhang W, Platel B, Karssemeijer N. Computer-aided detection of breast cancers using Haar-like features in automated 3D breast ultrasound. Medical physics 2015; 42:1498–504. [PubMed: 25832040]

Tan T, Platel B, Twellmann T, van Schie G, Mus R, Grivegnee A, Mann RM, Karssemeijer N. Evaluation of the effect of computer-aided classification of benign and malignant lesions on reader performance in automated three-dimensional breast ultrasound. Academic radiology 2013; 20:1381–8. [PubMed: 24119350]

Tang AM, Kacher DF, Lam EY, Wong KK, Jolesz F, Yang ES. Simultaneous ultrasound and MRI system for breast biopsy: compatibility assessment and demonstration in a dual modality phantom. IEEE transactions on medical imaging 2008; 27:247–54. [PubMed: 18334446]

Tejerina Bernal A, Tejerina Bernal A, Rabadan Doreste F, De Lara Gonzalez A, Rosello Llerena JA, Tejerina Gomez A. Breast imaging: how we manage diagnostic technology at a multidisciplinary breast center. Journal of oncology 2012; 2012:213421. [PubMed: 22829820]

Tilanus-Linthorst MM, Obdeijn IM, Bartels KC, de Koning HJ, Oudkerk M. First experiences in screening women at high risk for breast cancer with MR imaging. Breast cancer research and treatment 2000; 63:53–60. [PubMed: 11079159]

Torre LA, Bray F, Siegel RL, Ferlay J, Lortet-Tieulent J, Jemal A. Global cancer statistics, 2012. CA: a cancer journal for clinicians 2015; 65:87–108. [PubMed: 25651787]

Tozaki M, Fukuma E. Category assessment based on 3D volume data acquired by automated breast ultrasonography. Japanese journal of radiology 2012; 30:185–91. [PubMed: 22180186]

Tozaki M, Isobe S, Fukuma E. Preliminary study of ultrasonographic tissue quantification of the breast using the acoustic radiation force impulse (ARFI) technology. European journal of radiology 2011; 80:e182–7. [PubMed: 21788111]

Uematsu T, Kasami M, Yuen S. Comparison of FDG PET and MRI for evaluating the tumor extent of breast cancer and the impact of FDG PET on the systemic staging and prognosis of patients who are candidates for breast-conserving therapy. Breast cancer (Tokyo, Japan) 2009; 16:97–104.

Valente SA, Levine GM, Silverstein MJ, Rayhanabad JA, Weng-Grumley JG, Ji L, Holmes DR, Sposto R, Sener SF. Accuracy of predicting axillary lymph node positivity by physical examination, mammography, ultrasonography, and magnetic resonance imaging. Annals of surgical oncology 2012; 19:1825–30. [PubMed: 22227922]

Vallone P, D'Angelo R, Filice S, Petrosino T, Rinaldo M, De Chiara A, Gallipoli A. Color-doppler using contrast medium in evaluating the response to neoadjuvant treatment in patients with locally advanced breast carcinoma. Anticancer research 2005; 25:595–9. [PubMed: 15816633]

Vedantham S, Karellas A, Emmons MM, Moss LJ, Hussain S, Baker SP. Dedicated breast CT: Geometric design considerations to maximize posterior breast coverage. Physics in medicine and biology 2013; 58:4099–118. [PubMed: 23685899]

Vedantham S, Shi L, Karellas A, O'Connell AM, Conover DL. Personalized estimates of radiation dose from dedicated breast CT in a diagnostic population and comparison with diagnostic mammography. Physics in medicine and biology 2013; 58.

Venkatesh SS, Levenback BJ, Sultan LR, Bouzghar G, Sehgal CM. Going beyond a First Reader: A Machine Learning Methodology for Optimizing Cost and Performance in Breast Ultrasound Diagnosis. Ultrasound in medicine & biology 2015; 41:3148–62. [PubMed: 26354997]

Veronesi U, Paganelli G, Viale G, Luini A, Zurrida S, Galimberti V, Intra M, Veronesi P, Robertson C, Maisonneuve P, Renne G, De Cicco C, De Lucia F, Gennari R. A randomized comparison of sentinel-node biopsy with routine axillary dissection in breast cancer. The New England journal of medicine 2003; 349:546–53. [PubMed: 12904519]

Wan CF, Du J, Fang H, Li FH, Zhu JS, Liu Q. Enhancement patterns and parameters of breast cancers at contrast-enhanced US: correlation with prognostic factors. Radiology 2012; 262:450–9. [PubMed: 22282183]

Wang H-Y, Jiang Y-X, Zhu Q-L, Zhang J, Dai Q, Liu H, Lai X-J, Sun Q. Differentiation of benign and malignant breast lesions: a comparison between automatically generated breast volume scans and handheld ultrasound examinations. European journal of radiology 2012; 81:3190–200. [PubMed: 22386134]

Wang Y, Wang W, Li J, Tang J. Gray-scale contrast-enhanced ultrasonography of sentinel lymph nodes in a metastatic breast cancer model. Academic radiology 2009; 16:957–62. [PubMed: 19427801]

Warner E, Messersmith H, Causer P, Eisen A, Shumak R, Plewes D. Systematic review: using magnetic resonance imaging to screen women at high risk for breast cancer. Annals of internal medicine 2008; 148:671–79. [PubMed: 18458280]

Warner E, Plewes DB, Hill KA, Causer PA, Zubovits JT, Jong RA, Cutrara MR, DeBoer G, Yaffe MJ, Messner SJ, Meschino WS, Piron CA, Narod SA. Surveillance of BRCA1 and BRCA2 mutation carriers with magnetic resonance imaging, ultrasound, mammography, and clinical breast examination. Jama 2004; 292:1317–25. [PubMed: 15367553]

Warner E, Plewes DB, Shumak RS, Catzavelos GC, Di Prospero LS, Yaffe MJ, Goel V, Ramsay E, Chart PL, Cole DE, Taylor GA, Cutrara M, Samuels TH, Murphy JP, Murphy JM, Narod SA. Comparison of breast magnetic resonance imaging, mammography, and ultrasound for surveillance of women at high risk for hereditary breast cancer. Journal of clinical oncology : official journal of the American Society of Clinical Oncology 2001; 19:3524–31. [PubMed: 11481359]

Watermann DO, Foldi M, Hanjalic-Beck A, Hasenburg A, Lughausen A, Prompeler H, Gitsch G, Stickeler E. Three-dimensional ultrasound for the assessment of breast lesions. Ultrasound in obstetrics & gynecology : the official journal of the International Society of Ultrasound in Obstetrics and Gynecology 2005; 25:592–8.

Weinreb JC, Newstead G. MR imaging of the breast. Radiology 1995; 196:593–610. [PubMed: 7644617]

Wenkel E, Heckmann M, Heinrich M, Schwab SA, Uder M, Schulz-Wendtland R, Bautz WA, Janka R. Automated breast ultrasound: lesion detection and BI-RADS classification--a pilot study. RoFo : Fortschritte auf dem Gebiete der Rontgenstrahlen und der Nuklearmedizin 2008; 180:804–8. [PubMed: 18704878]

Wienbeck S, Fischer U, Perske C, Wienke A, Meyer HJ, Lotz J, Surov A. Cone-beam Breast Computed Tomography: CT Density Does Not Reflect Proliferation Potential and Receptor Expression of Breast Carcinoma()(). Translational Oncology 2017; 10:599–603. [PubMed: 28666188]

Wienbeck S, Lotz J, Fischer U. Review of clinical studies and first clinical experiences with a commercially available cone-beam breast CT in Europe. Clinical imaging 2017; 42:50–59. [PubMed: 27875762]

Wojcinski S, Gyapong S, Farrokh A, Soergel P, Hillemanns P, Degenhardt F. Diagnostic performance and inter-observer concordance in lesion detection with the automated breast volume scanner (ABVS). BMC medical imaging 2013; 13:36. [PubMed: 24219312]

Xin L, Chen L, Zhang H, Liu Q, Xu L, Wang B, Li T, Duan X, Liu Y. [Analysis of detecting value of ultrasound and the clinic-pathological features of axillary metastasis in breast cancer]. Zhonghua wai ke za zhi [Chinese journal of surgery] 2014; 52:924–8.

Yamamoto S, Maeda N, Tamesa M, Nagashima Y, Suga K, Oka M. Sentinel Lymph Node Detection in Breast Cancer Patients by Real-Time Virtual Sonography Constructed With Three-Dimensional Computed Tomography-Lymphography. The breast journal 2010; 16:4–8. [PubMed: 19825001]

Yamamoto S, Maeda N, Tamesa M, Nagashima Y, Yoshimura K, Oka M. Prospective ultrasonographic prediction of sentinel lymph node metastasis by real-time virtual sonography constructed with

three-dimensional computed tomography–lymphography in breast cancer patients. Breast cancer (Tokyo, Japan) 2012; 19:77–82.

Zhang X, Wu F, Han P. The role of (18)F-FDG PET/CT in the diagnosis of breast cancer and lymph nodes metastases and micrometastases may be limited. Hellenic journal of nuclear medicine 2014; 17:177–83. [PubMed: 25526754]

Zhang Y-N, Wang C-J, Xu Y, Zhu Q-L, Zhou Y-D, Zhang J, Mao F, Jiang Y-X, Sun Q. Sensitivity, Specificity and Accuracy of Ultrasound in Diagnosis of Breast Cancer Metastasis to the Axillary Lymph Nodes in Chinese Patients. Ultrasound in medicine & biology 2015; 41:1835–41. [PubMed: 25933712]

Zhao H, Xu R, Ouyang Q, Chen L, Dong B, Huihua Y. Contrast-enhanced ultrasound is helpful in the differentiation of malignant and benign breast lesions. European journal of radiology 2010; 73:288–93. [PubMed: 19559551]

Zhong Li-yao ZP, Rui-zhen Li,ze-min Cao,Jun-hui Wu The value of ultrasound contrast agents ingected subcutaneously for diagnosing sentinel lymph nodes of breast cancer. Chinese Journal of Ultrasonography 2007; 16:770–2.
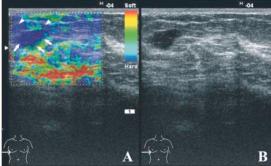
Figure 1.
Elastography could help to define the biopsy location and characterize a complex lesion. The two, left Figures, i.e. the SE image (A) and B-mode USG image (B), show a hypoechoic circumscribed lesion that is predominantly elastic and displays a mosaic pattern of green and blue. This was a fibroadenoma with a Tsukuba elasticity score of 2 and an SR of 1.76. The two, right figures, i.e. SE image (A) and B-mode USG image (B) -- the lesion (arrows), and the surrounding tissue (arrowhead) were colored blue and had an elasticity score of 5. Pathology revealed an invasive ductal carcinoma. Reprinted from (Gheonea, et al. 2011).
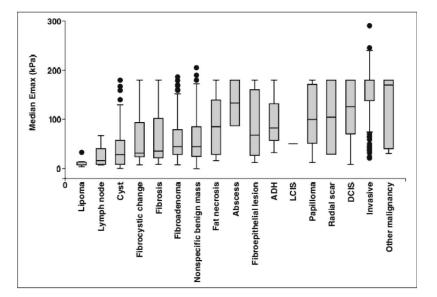
Figure 2.
Shear-Wave Stiffness of Breast Masses. The box-and-whisker plot of the median, maximum stiffness (termed "Emax") on shear-wave elastography (horizontal lines in bars) as the function of the histopathologic diagnosis for 1562, sonographically visible breast masses. The boxes represent the interquartile ranges (IQRs [25th–75th percentiles]), and the whiskers represent the 1.5-times IQR. Values outside whiskers are plotted as individual dots. ADH = atypical ductal hyperplasia, LCIS = lobular carcinoma in situ, DCIS = ductal carcinoma in situ. Reprinted from (Berg, et al. 2015).
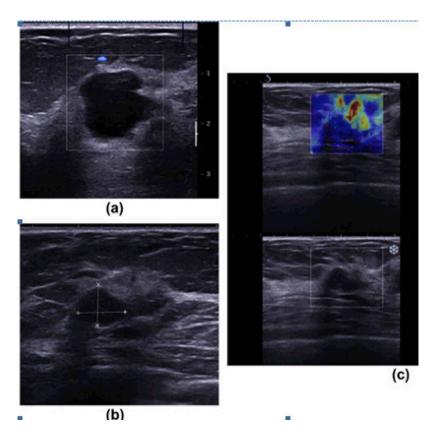
Figure 3.
Shear-wave elastography in the diagnosis of symptomatic, invasive, lobular breast cancer. A 47-year-old woman who had undergone a previous left mastectomy for ductal carcinoma *in situ* (DCIS), presented with a new lump in her right breast. (a) Ultrasound demonstrates benign cysts. (b) A well-defined, round lesion with posterior enhancement and mildly echogenic contents was thought to represent a thick cyst on grayscale ultrasound, but (c) SWE shows increased stiffness at and around the lesion (mean elasticity of 147 kPa). Subsequent biopsy and surgery confirmed a grade 2 ILC. Reprinted from (Sim, et al. 2015).
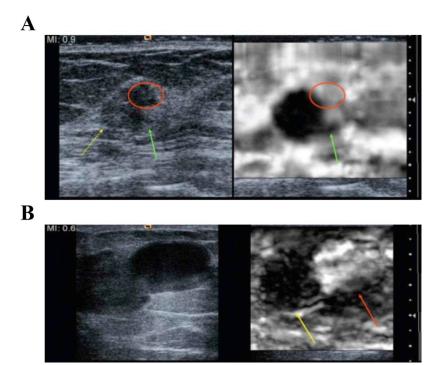
Figure 4.
Close evaluation of the elasticity patterns of a lesion can be helpful in their characterization and helpful in biopsy planning. A: Invasive ductal carcinoma with an area (red circle) that is "soft" on the elastogram. On pathologic examination from surgical resection, the soft area was a benign fibroadenoma, and which was not distinguishable from the invasive ductal carcinoma (yellow arrow) diagnosed in a 53 -year-old patient from the B-mode image. A spicule (green arrow) of the tumor is better seen on the elastogram. B: Images from an 85 - year-old patient who presented with a bloody nipple discharge. On the B-mode image, there is a large, complex lesion. On the elastogram, it is possible to identify a hard component (yellow arrow) and a soft component (red arrow). On pathologic examination, the solid component was a papillary carcinoma and the soft area was old blood. Reprinted from (Barr 2012).
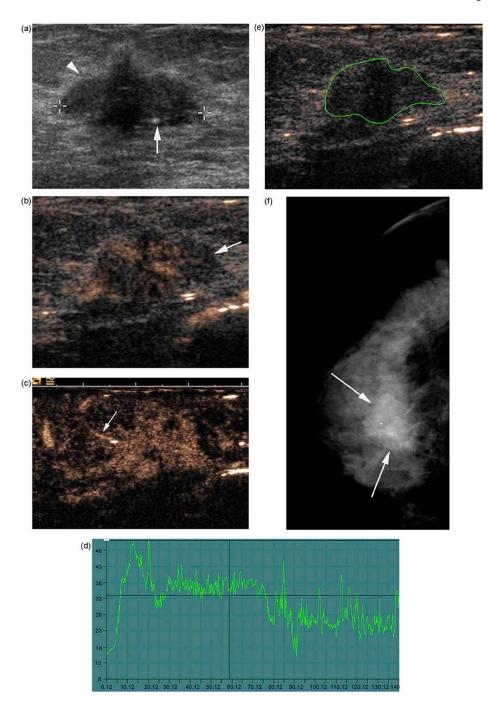
Figure 5.
Contrast US before and after contrast medium injection in a 66-year-old woman with 23–mm, ductal, infiltrative carcinoma. (a) B mode sonography. (b) In the contrast mode (SonoVue ®) with Coherence Pulse Sequencing and B mode, the tumor is strongly enhanced after injection. Vessels are located in the peripheral area of the lesion. (c) In the contrast mode with Coherence Pulse Sequencing only, the tumoral-feeding artery is visible outside of the lesion (arrows). (d) Dynamic curve of enhancement after injection. Enhancement is fast, i.e. the delay of peak enhancement = 10 s, and with a wash-out phase (total time: two min).

(e) Region of interest (ROI) on the tumor to obtain enhancing curves. (f) Mammogram. Cranio-caudal view of the right breast. Reprinted from (Balleyguier, et al. 2009)
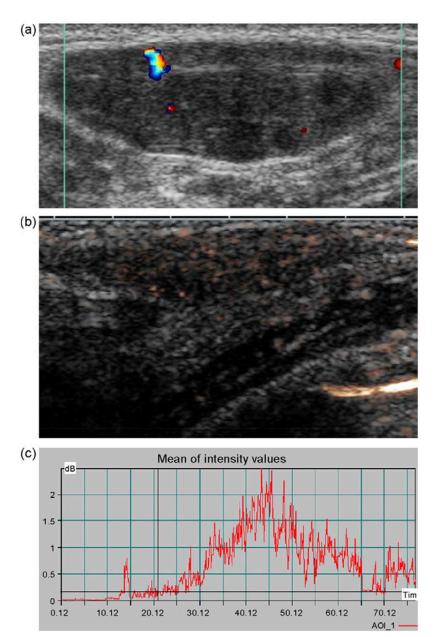
Figure 6.
Contrast-enhanced ultrasound of a 22-year-old woman with adenofibroma. (a) Color Doppler. Smooth contours, homogeneous content, and posterior enhancement are criteria for benignity. (b) Contrast US (SonoVue ®) with Coherence Pulse Sequencing as well as thin and multiple arterial vessels are visible in the center of the lesion. Global enhancement is moderate and homogeneous. These enhancement parameters are suggestive of a benign lesion. (c) Enhancement curve. Enhancement is delayed compared with that of malignant tumors (>20 s). The enhancement value is also moderate compared with that of malignant carcinoma. The wash-out phase is longer. Reprinted from (Balleyguier, et al. 2009).
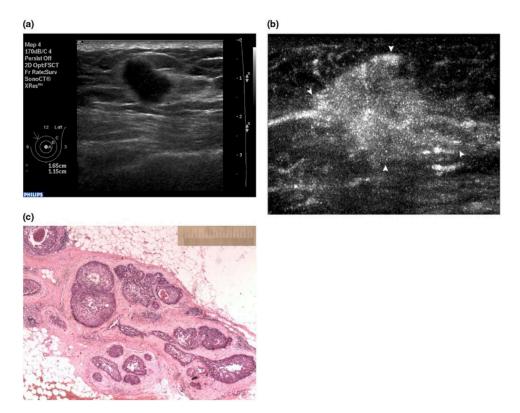
Figure 7.
Comparison of conventional ultrasound and contrast-enhanced ultrasound in a 47-year-old woman with a mass pathologically verified as low-grade DCIS. (a) Conventional US: a mass of 17×12 mm surrounded by a hyperechoic halo. (b) MVI: the mass shows diffuse enhancement (arrow head) and its size increases to 22×16 mm. Large, enhancing blood vessels were not included in the measurement. (c) Photography of the histopathological specimen (hematoxylin-eosin stain, original magnification ×20): the difference in size corresponds to the extent of intraductal carcinoma. Reprinted from (Jiang, et al. 2007).
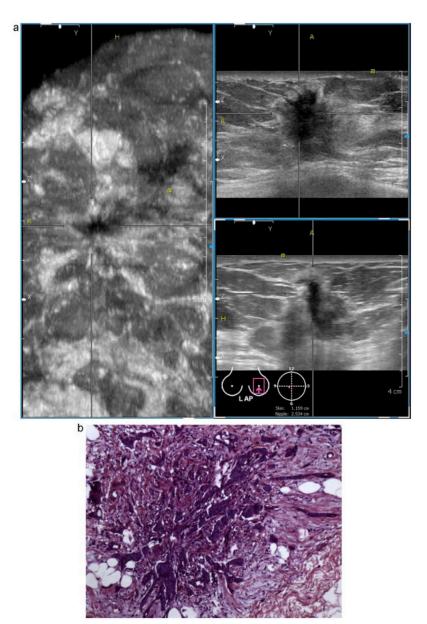
Figure 8.
(a) Automated breast volume scanning image of infiltrating ductal carcinoma. Note the heterogeneous echogenicity, spiculated border, indistinct margin, and "taller than wide" appearance. (b) Histopathology image of the same mass. Note the infiltration of ill-defined glands into the surrounding collagenous stroma. Reprinted from (Wang, et al. 2012).

Figure 9.
Automated breast volume scanner: (A) Acuson S2000 ABVS (Siemens Medical Solutions). The transducer plate (B) is positioned over the breast and an automated scan is performed in order to obtain a series of two-dimensional images. Depending on the breast size, more than three scans per breast may be required. Reprinted from (Shin, et al. 2015).
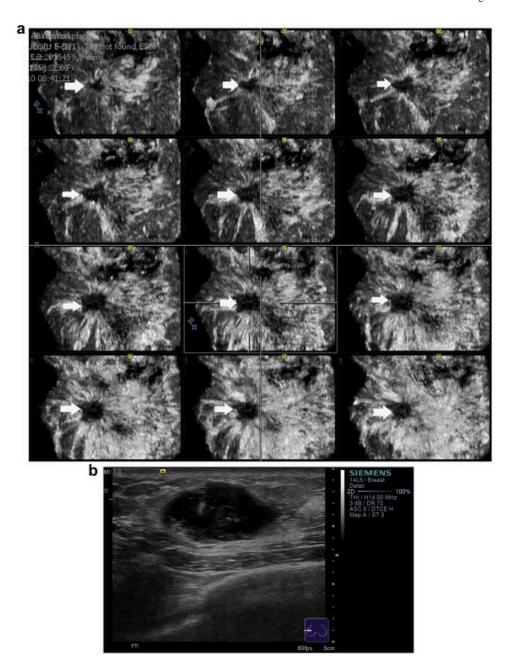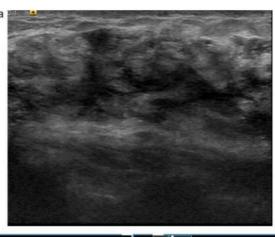
Figure 10.
(a) Automated breast volume scanner images of an invasive ductal carcinoma of the breast in a multislice view from the skin down to the thoracic wall in the coronal plane (the slices are 0.5 mm). (b) Handheld B- mode ultrasound. The typical retraction phenomenon of the mass is observed in several, consecutive coronal planes (arrowhead on the right).This indicates the conditions of the masses at different depths. Reprinted from (Chen, et al. 2013).
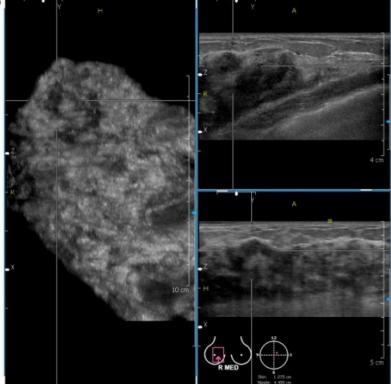
Figure 11.
Automatically generated breast volume scan of diffuse, multiple, invasive ductal carcinomas in a 29-year-old woman. (a) HHUS showed a diffuse, hypoechoic area in almost the entire right breast and that was misinterpreted as adenosis. (b) Three-dimensional, ABVS multiplanar images showing the same area. This lesion was extensive (the diameter was 6.5 cm), although the margin between the tumor and the surrounding, normal parenchyma could be revealed with ABVS because of the wide scanning area. Reprinted from (Wang, et al. 2012).
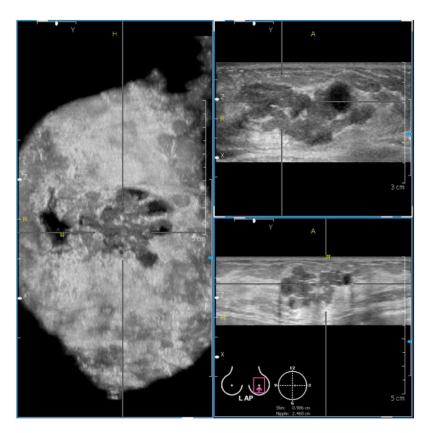
Figure 12.
Automatically generated breast volume scan of an 11-year-old girl with a palpable mass (intraductal papilloma) in the left breast. These showed three orthogonal planes of the anterior–posterior left breast, i.e. coronal reconstruction (left image), axial original plane (upper right image), and sagittal reconstruction (lower right image). In the coronal plane, dilated lactiferous ducts can be detected and the intraluminal echoes can be demonstrated. Reprinted from (Wang, et al. 2012).
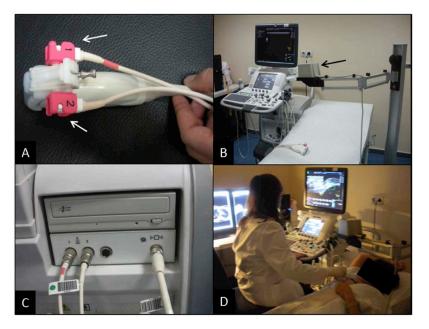
Figure 13.
US and the RtMR-US system. (a) Electromagnetic sensors on the tip of the probe (white arrows). (b) Electromagnetic transmitter (black arrow). (c) Connection unit between the lector magnetic transmitter, sensors, and the navigation system. (d) RtMR-US examination after co-registration. Reprinted from (Pons, et al. 2014).

Figure 14.
Glandular tissue and a Cooper's ligament are shown at the confluence of the upper quadrant of the right breast. Live US (white arrow) using the volume navigation technique using a late phase of contrast-enhanced MR (white arrowhead) are both able to image the morphology with sharp anatomical detail. Due to the smaller magnification of the MR image, a green box is electronically displayed on the MR image, showing the US scan area. Reprinted from (Fausto, et al. 2012).
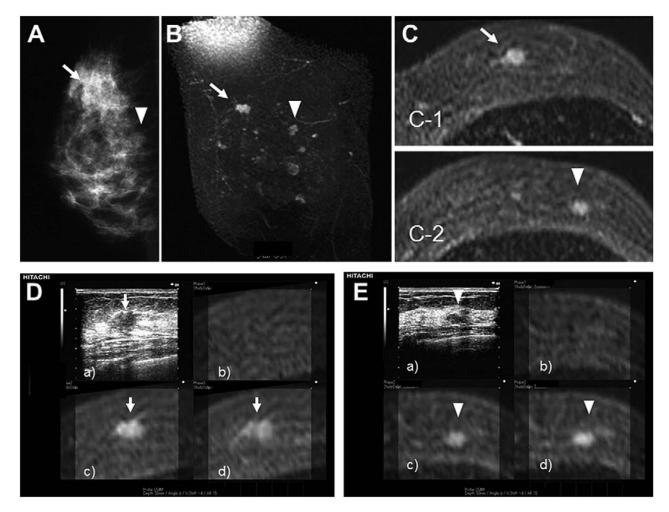
Figure 15.
A 43-year-old patient with architectural distortion and a mass in the right breast. (A) Mammography shows architectural distortion (arrow) and a well-circumscribed mass (arrowhead) on the mediolateral oblique films. (B) Coronal T1-weighted, contrast-enhanced MRI. (C) Transverse images show an irregularly shaped, margined, 12-mm mass diagnosed as invasive ductal carcinoma (arrow:c-1) as well as an oval-shaped, smooth-margined, 8-mm mass that had not been identified on conventional B-mode (arrowhead:c-2). (D) RVS shows the 12-mm, irregularly shaped mass that is taller than it is wide (a), and corresponding to the MRI lesion (b–d) (arrow). The precontrast MRI image (b) used to identify lesions in the absence of T1-weighted signals before enhancement is necessarily in the image plane displayed by the RVS system. Histopathological analysis of the sonographically guided, core biopsy samples was consistent with invasive ductal carcinoma. (E) RVS shows the 8-mm, oval mass that is wider than it is tall (a), and corresponding to the MRI lesion (b–d) (arrowhead). A histopathological analysis of sonographically guided core biopsy samples indicated that this tumor was a fibroadenoma. Reprinted from (Nakano, et al. 2012).

Table 1.

Characteristics of the sonogram evaluation of breast cancer (Chen, et al. 2013) (Gokhale 2009).

Lexicon	Malignant tumors	Benign tumors
Shape	Irregular	Oval, round
Orientation	Vertical, taller than wide, indifferent	Parallel, wider than tall
Margin	Indistinct	Circumscribed, identifiable, thin echogenic capsule
Margin contour	Irregular, angular, spiculate	Smooth, three or fewer gentle lobulations
Echogenicity	Markedly hypoechoic	Hyperechoic, isoechoic or mildly hypoechoic
Genity	Homogeneous	Heterogeneous
Posterior features	Shadowing	Enhancement, no changes
Calcification	Microcalcification	Absent
Surrounding tissue	Architectural distortion	Compression, no alteration
Retraction phenomena	Present	Absent

Table 2.

Relative risk (RR) of breast-cancer mortality with Mammography Screening

Author/Year	Accrual period	Study recruitment	Relative risk of breast-cancer mortality 50 years (Age, RR)	Relative risk of breast-cancer mortality <50 years (Age, RR)
(Nystrom, et al. 2002)	Up to 1996	247010 women Invited group 129750, Control group 117260	50–54y, 55–59y, 60–64y, 65–69y RR=0.95,0.76, 0.68, 0.69, respectively	-
(Bastardis-Zakas, et al. 2010)	1988–2006	Meta-analyses of eight randomized control trials	-	40–49y RR=0.81
(Moss, et al. 2006)	1963–1990	160,921 women	-	40–49y RR= 0.83 [95% CI 0·66–1·04], p=0.11
(Humphrey, et al. 2002)	1963–1982	Reviewed 154 publications from ten trials	50 y RR= 0.78 (95%CI, 0.70 to 0.87)	< 50 y RR=0.85 95%CI, 0.73 to 0.99)
(Nelson, et al. 2009)	1986–2006	Meta-analysis of seven Mammography Screening Trials	50–59y RR=0.86 (0.75–0.99) 60–69y RR= 0.68 (0.54–0.87)	39–49y RR=0.85(0.75–0.96
(Donna Fitzpatrick-Lewis 2011)	2008–2010	Systematic review Randomized controlled trials	50–69y seven studies RR=0.79(0.68–0.90) 70y two trials RR=0.68(0.45–1.01)	Eight trials 39–49y RR=0.85 (0.75–0.96) two trials 39–49y RR=0.97(0.91–1.04)
(Miller, et al. 2014)	1980–85 25-year- follow up	89,835 women Randomized controlled trials	40–59y hazard ratio 1.05 (0.85 to 1.30) The findings for women aged 40–49 and 50–59 were almost identical	
(Hamashima, et al. 2015)	1985 – 2014	Randomized controlled trials on PubMed and other databases	40–74 years without clinical breast examination RR=0.75 40–64 years with clinical breast examination RR= 0.87	

Author Manuscript

Author Manuscript

Author Manuscript

Author Manuscript

Table 3.

Diagnostic performance of multimodality imaging in breast cancer (Sensitivity and Specificity)

Author Year	Accrual period	Subject number of research	Mammography	US	MRI	PET
BCSC data through 2009 (Consortium)	2004–2008	363,048 Diagnostic Mammography Examinations	SE=84.4% SP=91.3%	-	-	-
(Kolb, et al. 2002)	1995–2000	11,130 asymptomatic mean age,63.7 years	total SE=77.6% 49y SE=58% >50y SE=82.7% total SP=98.8%	total SE=75.3% 49ySE=78.6% 50y SE=74% total SP=96.8%		
(Saarenmaa, et al. 2001)	1996–1997	572 breast cancer cases age groups 26–49. 50–59 and 60–92	SE=0.93% Increased by age, fattiness of breast OR=0.2,0.4	SE=0.86% Decreased by age OR=2.3 Increased by fattiness of the breast OR=O.S		
(Houssami, et al. 2003)	1994–1996	480 25–55 years 240 with breast cancer 240 age-matched women not having cancer	total SE=75.8% 45ySE=71.7% 46–55 fr- SE=79,1% total SP =87.6%	total SE=81.7% 45 v SE=84.9% 46–55y SE=79.1% total SP =88.0%		
(Shen, et al. 2015)	2008–2010	13 339 high-nsk women 30–65 years	SE=57.1% SP =100% diagnostic accuracy =76.6% PPY=72.7%	SE=100% SP =99.9% diagnostic accuracy =99.9% PPV=70.0%		
(Berg, et al. 2004)	1999–2002	177 malignant foci in 121 cancerous breasts	SE=67.8% %SP =75%	SE=83.0% SP =34%	SE=94.4% SP =26%	-
(Kuhl, et al. 2005)	1996–2002 mean follow- up of 5.3	529 asymptomatic women who were suspected or proven to have a breast cancer susceptibility gene (3RCA)	SE=32.6% SP =96.8%	SE=39.5% SP =90.5%	SE=90.7% SP=97.2%	-
(Kuhl, et al. 2000)	1996–1998	192 asymptomatic women proven or suspected to be earners of a breast cancer susceptibility gene.	SE=33% PPV=30%	SE=33% PPV=12%	SE=100% PPY=64%	
(Leach, et al. 2005)	1997– 2004	649 patients with a strong family history of breast cancer or a high probability of a BRCA1. BRCA2. or TP53 mutation	SE=40% SP =93%		SE=77% SP =81%	

Author Year	Accrual period	Subject number of research	Mammography	US	MRI	PET
(Sardanelli. et al. 2011)	2000–2007	501 women with a high genetic nsk	SE=50% SP =99@.	SE=52% SP =98.4%	SE=91% SP=96.7%	
(Warner, et al. 2008)	Data bases 1995–2007	Summarized 11 studies that screened women at very high risk for breast cancer	SE=32% SP =94.7%		SE=75% SP=96.1%	
(Zhang, et aL 2014)	2006–2012	164 patients with invasive breast cancer	-	-	-	SE=86%
(Song, et al 2015)	2008–2012	86 patients with invasive breast cancer Detecting multifocality in breast cancer patients	SE=66.7% SP=89.5%	SE=83.3% SP=711%	SE=100% SP=61.8%	SE=33.3% SP=93.4 %
(Berg, et al 2011)	2006–2008	388 women with invasive and. or intraductal breast cancer			SE=80.7% SP=86.3% P PV=53%	For PEM SE=80.5% SP=91.2% PPY=66%
(Berg, et al. 2006)		94 consecutive women with known breast cancer				For PEM SE=90 SP=86 PPV=88 NPV=88 Accuracy=88

Table 4.

Diagnostic performance of multiple imaging modalities in breast lymph nodes

Author Year	Accrual period	Subject number of research	Mammography	US			MRI	PET
(Zhang, et al. 2015)	2010–2011	1.049 breast cancers	-	SE=69.4:SP=81.8:Accuracv=77			-	-
(Xin. et al. 2014)	2012–2013	323 female primary breast cancer		SE=35.6;SP=98.9;PPV=35.6;NPV=68.3				
(Alvarez, et al. 2006)	1980–2004	Meta analysis with Sixteen articles		Cnterion — Non-palpable — Palpable +non-palpable; size<5 mm: SE=48.8–87.7 SP=55.6–97.3 / SE=66.1–72.7 SP=44.1–97.9; morphology: SE=26.4–75.9 SP=S5.4–98.1 / SE=54.7–92.3 SP=S0.4–87.1			-	-
(Valente, et al. 2012)	200S-2010	244 invasive breast carcinomas	SE = 21 SP= 99.5	SE=43.5 SP= 96.2			SE=37.1 SP= 96.7	-
(Heusner. et al. 2009)	2007–2008	61 patients with breast cancer						FDG PET/CT SE=5S:SP=92 PPV=82:NPV=77 Accuracy=79
(Kvistad. et al. 2000)	1998	65 patients with invasive breast cancer					SE=83 SP= 90 Accuiac=88	
(Lind. et al. 2004)	Review of 1989–2004	201						For local récurrence, lymph node métastasés and distant métastasés SE =96%:SP = 77%
(Song, et al. 2015)	2008-2012	86 invasive breast cancer	SE = 36.4 SP =S6.8	SE = 61.4 SP =92.1			SE = 61.4 SP =73.7	FDG-PET SE = 47.7; SP =81.6
(Heusner. et al. 2008)		40 women with suspected breast cancer						18F-FDG PET/CT SE = 0.80
(An. et al. 2015)	2008-2012	37 patients with breast cancer. For internal mammary LN		Initial US SE=76.6 Initial US combined with SLUS SE=96.7				SE=92.9

Author Year	Accrual period	Subject number of research	Mammogra phy	US	MRI	PET
		metastasis				